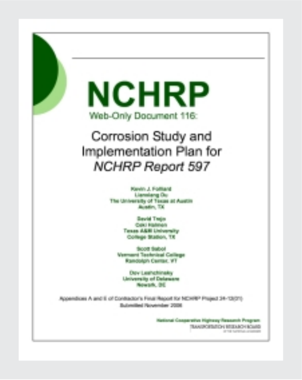

NCHRP
Web-Only Document 116:

Corrosion Study and
Implementation Plan for
NCHRP Report 597

Corrosion Study and Implementation Plan for NCHRP Report 597

DETAILS

0 pages | null | PAPERBACK
ISBN 978-0-309-43615-1 | DOI 10.17226/23119

AUTHORS

ACKNOWLEDGMENT

This work was sponsored by the American Association of State Highway and Transportation Officials (AASHTO), in cooperation with the Federal Highway Administration, and was conducted in the National Cooperative Highway Research Program (NCHRP), which is administered by the Transportation Research Board (TRB) of the National Academies.

COPYRIGHT PERMISSION

DISCLAIMER

THE NATIONAL ACADEMIES

Advisers to the Nation on Science, Engineering, and Medicine

The **National Academy of Sciences** is a private, nonprofit, self-perpetuating society of distinguished scholars engaged in scientific and engineering research, dedicated to the furtherance of science and technology and to their use for the general welfare. On the authority of the charter granted to it by the Congress in 1863, the Academy has a mandate that requires it to advise the federal government on scientific and technical matters. Dr. Ralph J. Cicerone is president of the National Academy of Sciences.

The **National Academy of Engineering** was established in 1964, under the charter of the National Academy of Sciences, as a parallel organization of outstanding engineers. It is autonomous in its administration and in the selection of its members, sharing with the National Academy of Sciences the responsibility for advising the federal government. The National Academy of Engineering also sponsors engineering programs aimed at meeting national needs, encourages education and research, and recognizes the superior achievements of engineers. Dr. Charles M. Vest is president of the National Academy of Engineering.

The **Institute of Medicine** was established in 1970 by the National Academy of Sciences to secure the services of eminent members of appropriate professions in the examination of policy matters pertaining to the health of the public. The Institute acts under the responsibility given to the National Academy of Sciences by its congressional charter to be an adviser to the federal government and, on its own initiative, to identify issues of medical care, research, and education. Dr. Harvey V. Fineberg is president of the Institute of Medicine.

The **National Research Council** was organized by the National Academy of Sciences in 1916 to associate the broad community of science and technology with the Academy's purposes of furthering knowledge and advising the federal government. Functioning in accordance with general policies determined by the Academy, the Council has become the principal operating agency of both the National Academy of Sciences and the National Academy of Engineering in providing services to the government, the public, and the scientific and engineering communities. The Council is administered jointly by both the Academies and the Institute of Medicine. Dr. Ralph J. Cicerone and Dr. Charles M. Vest are chair and vice chair, respectively, of the National Research Council.

The **Transportation Research Board** is one of six major divisions of the National Research Council. The mission of the Transportation Research Board is to provide leadership in transportation innovation and progress through research and information exchange, conducted within a setting that is objective, interdisciplinary, and multimodal. The Board's varied activities annually engage about 7,000 engineers, scientists, and other transportation researchers and practitioners from the public and private sectors and academia, all of whom contribute their expertise in the public interest. The program is supported by state transportation departments, federal agencies including the component administrations of the U.S. Department of Transportation, and other organizations and individuals interested in the development of transportation. **www.TRB.org**

www.national-academies.org

Contents

This document contains Appendices A and E from the contractor's final report on NCHRP Project 24-12(01). The main body of the final report, including Appendices B through D, has been published as *NCHRP Report 597: Development of a Recommended Practice for Use of Controlled Low-Strength Material in Highway Construction*.

APPENDIX A
CORROSION STUDY

Introduction

Controlled low-strength material (CLSM) is a cementitious, flowable, material, commonly made with cement, supplementary cementitious materials (SCMs), and fine aggregate, specifically designed as a replacement for soil backfill. CLSM is commonly used as a backfill for trenches, often when these trenches are located in roadways and undergo repeated loadings from vehicular traffic. Potential benefits of using CLSM include faster backfilling of the trench, less labor required for placement, and decreased long-term settlement when compared with conventional soil backfill. Although the material has shown much promise, the use of CLSM is not as common as would be expected, considering these potential benefits.

A major challenge in implementing the use of CLSM is the lack of knowledge on the material in the concrete materials and construction fields. Because CLSM often replaces conventional soils, many in the concrete industry believe geotechnical engineers should be researching, engineering, and promoting the use of this material. Alternatively, because the material uses cement as a binding agent, most geotechnical engineers believe CLSM should be researched, engineered, and promoted by concrete material engineers. Committee 229, *Controlled Low-Strength Materials*, of the American Concrete Institute (ACI) has taken the lead in generating data related to the use of this material. However, specifiers are reluctant to specify CLSM because limited data are available on the corrosion performance of metallic pipe materials embedded in CLSM. Existing guidelines on the effect of this material on the corrosivity and service-life of pipes are not available. Existing guidelines for determining the corrosivity of soil do not consider the unique characteristics of CLSM and, even though not specifically developed for cementitious materials (i.e., CLSM), often indicate that CLSM could be detrimental to the corrosion performance of pipes embedded in CLSM.

It has been well established in the literature that the high pH of the pore solution in cementitious materials and the reduced permeability and diffusivity of these cementitious materials, when compared with conventional backfill materials, provides improved corrosion protection for embedded metallic materials. But, these characteristics have not yet been considered in existing CLSM guidelines and standards. As such, there is a need to either validate the applicability of existing guidelines and standards for the corrosion performance and protection of pipe embedded in soils for pipes embedded in CLSM or to develop new, more appropriate guidelines for the corrosion performance of metallic pipe embedded in CLSM.

Several methods have been developed to evaluate the need for additional protection and the service life of pipes embedded in conventional soil backfill. Probably two of the most commonly used standards for corrosion of metallic pipes in soils are ANSI/AWWA C105/A21.5, *American National Standard for Polyethylene Encasement for Ductile Iron Piping for Water and Other Liquids,* and California 643, *Method for Estimating the Service Life of Steel Culverts*. ANSI/AWWA C105/A21.5 assigns points for various soil backfill characteristics. If the sum of the points from all characteristics is more than 10, the soil is assumed to be corrosive and the pipe requires additional protection. Table 1 shows the assigned points for the various conditions in the

ANSI/AWWA standard. California 643 estimates the maintenance-free service life of galvanized steel culverts in soils based on the pH and minimum electrical resistivity of soils. Figure 1 shows the California 643 chart.

Table 1 Assigned points for various soil characteristics (ANSI/AWWA C105/A21.5).

Soil Characteristics	**Points**
Resistivity--ohm-cm (based on single probe at pipe depth or water saturated soil box)	
<700	10
700-1000	8
1000-1200	5
1200-1500	2
1500-2000	1
>2000	0
pH	
0.0-2.0	5
2.0-4.0	3
4.0-6.5	0
6.5-7.5	0*
7.5-8.5	0
>8.5	3
Redox potential	
>+100 mV	0
+ 50 to + 100 mV	3.5
0 to + 50 mV	4
Negative	5
Sulfides	
Positive	3.5
Trace	2
Negative	0
Moisture	
Poor drainage, continuously wet	2
Fair drainage, generally moist	1
Good drainage, generally dry	0
**If sulfides are present and low or negative redox potential results are obtained give three points for this range*	

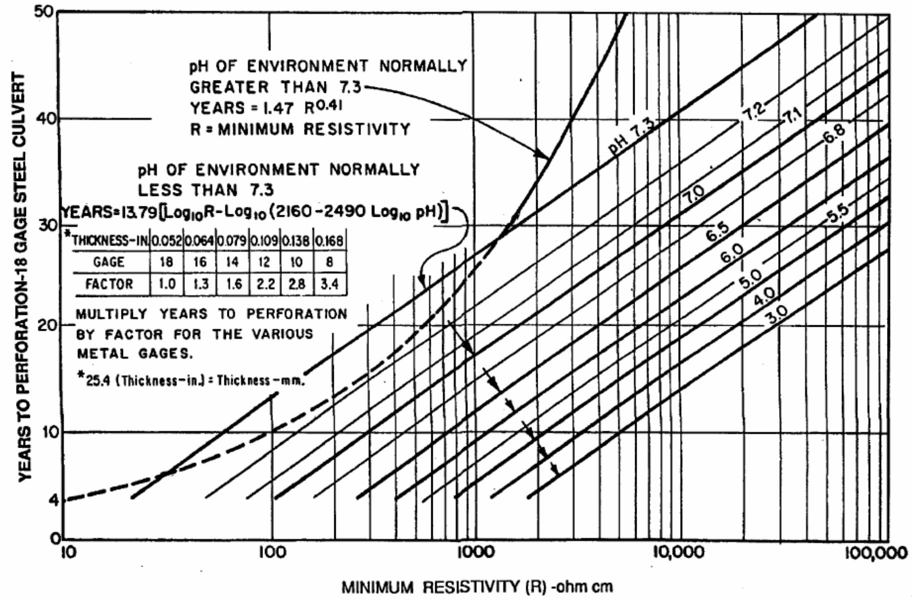

Figure 1 California 643 chart to estimate years to perforation of steel culverts.

Resistivity of the electrolyte can be an influencing parameter for most corroding systems. Peabody (1967), Coburn (1978), Palmer (1990), Chaker (1990), and Escalante (1992) all noted that as the soil resistivity increases, corrosion decreases. The ANSI/AWWA standard uses resistivity as a key contributing parameter for determining whether additional corrosion protection is required. However, Abelleira et al. (1998) found that CLSM saturated with corrosive water had a resistivity of approximately one-third of the resistivity of sand, even though the corrosion rate was almost negligible for the steel samples embedded in the CLSM. As such, resistivity alone may not necessarily be a significant indicator of corrosion performance for metallic pipes embedded in CLSM.

The pH of soils is also identified as a key soil characteristic in the ANSI/AWWA standard and in the California 643 Method for evaluating soil corrosivity. The ANSI/AWWA standard notes that for a pH range from 0.0 to 4.0, the soil serves well as an electrolyte and can influence corrosion. Thus, lower pH values would be expected to result in higher corrosion rates and have higher assigned point values. For soils with pH values greater than 8.5, the standard notes that these soils are generally quite high in dissolved salts, resulting in lower resistivity values and higher assigned point values. But, the high pH of the CLSM results from the hydroxyl ions and alkalis present in the pore solution and not from dissolved salts. It has been well documented that high pH pore solutions result in stable, protective, passivating oxide films on iron products (Broomfield 1997). Thus, assigning 3 points for high pH values is probably not applicable for CLSM backfill.

Two other soil characteristics identified in the ANSI/AWWA standard are the oxidation-reduction (redox) potential and the sulfide content in the soil. The redox potential is a measure of the oxygen availability in the soil and provides an indication of whether sulfate-reducing bacteria could be present in the backfill material. Testing of select CLSM samples for the redox potential has shown that the redox potential is more positive than 100 mV, indicating that oxygen is available and sulfate reducing bacteria would not occur in these environments. This would be typical of most CLSM mixtures as these mixtures are purposely designed for low strength. Lower strength CLSM mixtures typically exhibit relatively high porosity and permeability values, providing oxygen relatively easy access to the internal CLSM microstructure. The presence of sulfides indicates that sulfate-reducing bacteria could be present. The availability of free sulfides (and sulfates) is expected to be low in the CLSM pore structure, indicating that the present of sulfate-reducing bacteria would be unlikely.

The last soil characteristic that could influence the corrosion of pipes is the moisture content of the backfill material. Bonds (1992) found that the moisture content of CLSM can increase by 4 orders of magnitude from a dry to saturated state. Although resistivity may not be a parameter that can solely predict the corrosion of pipe embedded in CLSM, water is necessary for corrosion reactions and moisture availability could influence the corrosion activity of the pipe. Completely dry conditions will eliminate corrosion. Higher moisture contents can lead to higher corrosion activity and the ANSI/AWWA standard allocates 2 points for continuously wet conditions.

In addition to these soil characteristics, exposing a pipe to different environments can result in the pipe having different corrosion potentials that, in turn, can result in accelerated corrosion at the interface of these two environments. If it is assumed that a metallic material is embedded in different materials A and B and the corrosion potential for the metal embedded in material A, $E_{corr,A}$, is more negative than the corrosion potential of the same material in material B, $E_{corr,B}$, the metal in material A will lose electrons to the metal in material B. In this case, the metal in material A is denoted as being more active than the metal in material B. In conditions where these different environmental conditions occur, if the difference in corrosion potentials is sufficient, the metal with the more active corrosion potential will be preferentially attacked via corrosion (in this case the metal in material A). Figure 2 shows a typical schematic of the electron flow and localized corrosion.

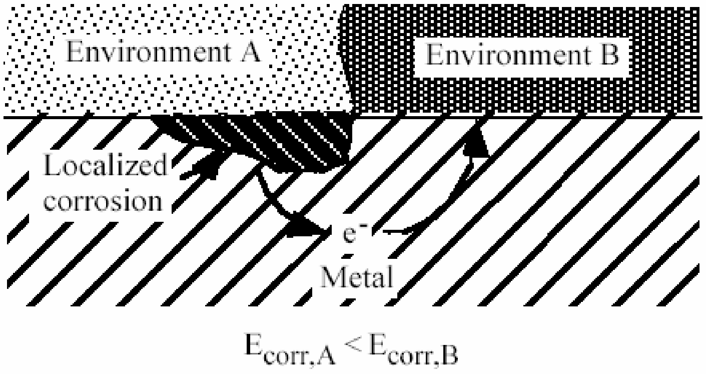

Figure 2 Electron flow leading to localized corrosion as a result of a metal being exposed to different environments.

In many instances when CLSM is used in the field, it may not be possible to embed a pipe entirely in CLSM. This could occur when a pipe undergoes localized repair or replacement and CLSM is used as a bedding and backfill material for the repaired area (scenario 1), when a pipe lateral crosses a trench that is to be backfilled with CLSM (scenario 2), or when CLSM is used only as a bedding material and conventional fill materials are used as the backfill material (scenario 3). Figure 3 shows these possible scenarios. In these scenarios, different environmental conditions around metallic pipes could generate galvanic corrosion cells that could lead to accelerated, localized corrosion and reduce life expectancies of the pipelines. Concern about the development of galvanic corrosion cells due to potential difference on ductile iron pipes in contact with CLSM and soils simultaneously has also been expressed by the Ductile Iron Pipe Research Association (DIPRA 1994).

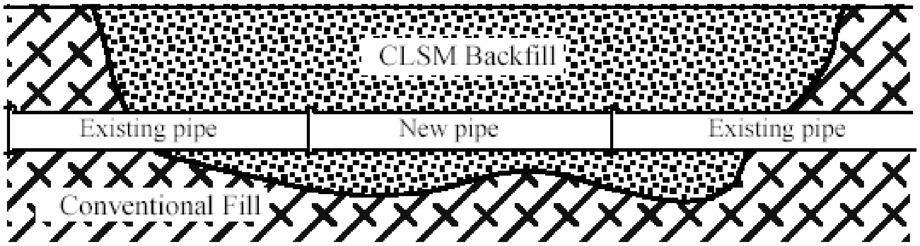

Elevation View - Scenario 1

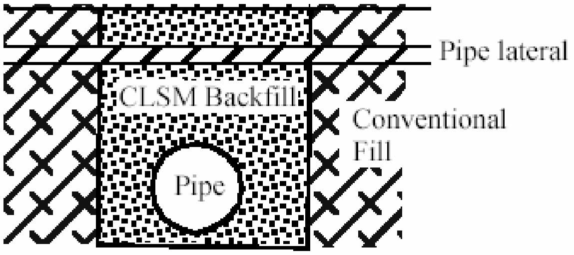

Cross Section View - Scenario 2

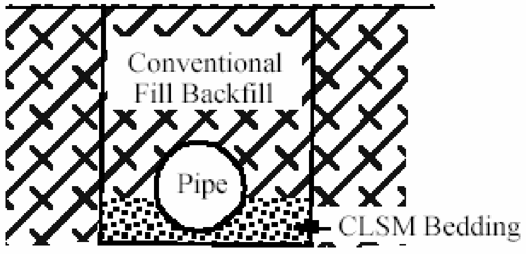

Cross Section View - Scenario 3

Figure 3 Various scenarios where pipe cannot be completely embedded in CLSM.

Extensive research has been performed on the corrosion performance of metallic pipelines embedded in different soil environments (Denison and Romanoff 1946, Romanoff 1957, Hoar and Farrer 1961, Levlin 1996). Results of these studies indicate that corrosion due to the potential difference on metallic materials in contact with different soils enhances the corrosion process and deterioration rate. Researchers also investigated the corrosion of steel reinforcement in concrete, due to the differences in the surrounding concrete environment, such as differential aeration, differential moisture content, differential salt concentrations, etc. (Mozer et al. 1965). However, there has only been limited research investigating the corrosion of metallic materials in contact with a cementitious material (e.g. CLSM) and a soil simultaneously. Sarhan et al. (2002) performed a study on drilled concrete shafts with flaws (voids or soil inclusions) investigating the effects of two different pH environments (soil and concrete) on the corrosion of reinforcement steel. The authors reported that the corrosion rate of the exposed steel was increased by 3.3 to 5.6 times.

Engineers commonly use the ANSI/AWWA standard and the California 643 Method to determine the corrosivity of soils for metallic pipe applications. Engineers also use these standards for evaluating the corrosivity of other materials and other applications. Because CLSM is a cementitious material, these standards for evaluating soils are likely not applicable for this material. However, engineers currently have no guidance on how to evaluate the corrosivity of CLSM for pipe applications and these standards are commonly used. Because these standards are likely not applicable for CLSM, they may be limiting the use of CLSM for backfill applications. As a result, the researchers developed a research program to evaluate the effect of CLSM on the corrosion performance of ductile iron pipe and galvanized steel and also to evaluate the potential impact of embedding these materials in different environments, both CLSM and soils.

Research Significance

The cost of corrosion exceeds $7 billion for gas and liquid transmission pipelines, $36 billion for drinking water and sewer systems, and $5 billion for gas distribution pipelines annually (FHWA-RD-01-156 2001). Even though CLSM has many inherent advantages, this material is not being specified and used as much as would be expected because limited data are available on how CLSM influences the corrosion performance of these metallic pipes. This paper presents results of a research program investigating the influence of CLSM on the corrosion performance of ductile iron pipe and galvanized steel pipe embedded in various different CLSM mixtures. These data can be used to better understand the influence of CLSM on the corrosion activity of metallic pipe materials such that engineers can make informed decisions regarding the applicability of CLSM for pipe bedding and backfill applications.

Sample Fabrication, Materials, and Mixture Proportions

To evaluate their corrosion performance, metallic coupons machined from ductile iron and galvanized steel pipes were embedded in CLSM and soils and tested in two conditions; uncoupled and coupled. Figure 4a and 4b shows the samples for both uncoupled and coupled conditions.

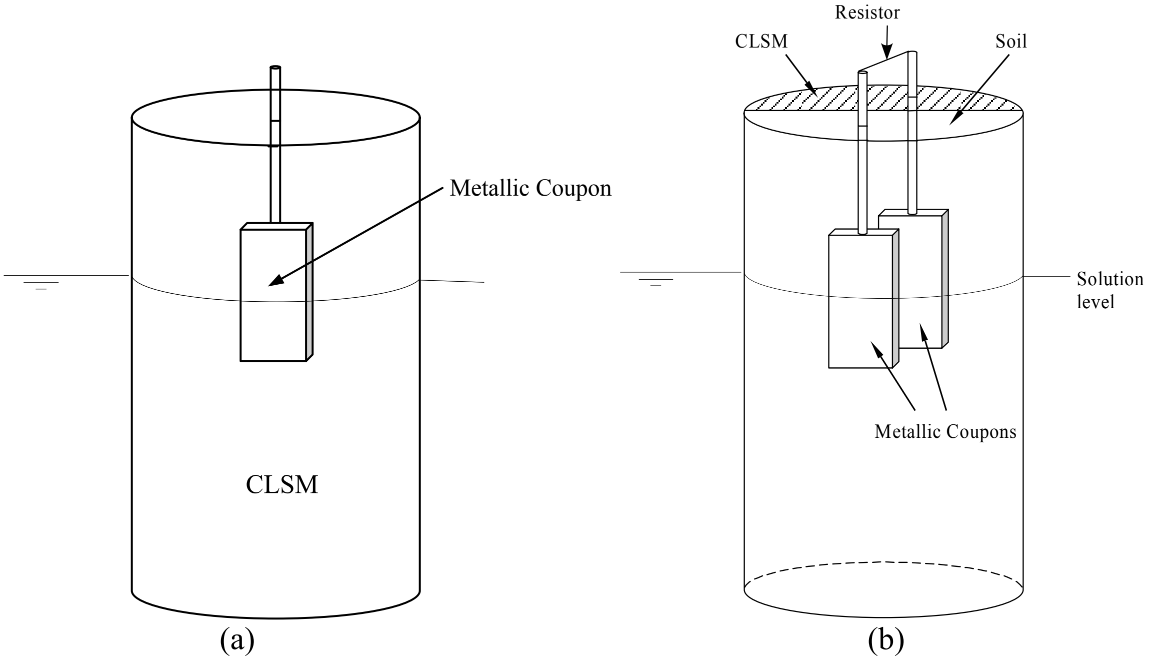

Figure 4 a) Uncoupled Sample b) Coupled Sample

Metallic coupons in the uncoupled state were embedded in 75 x 150 mm plastic cylinders containing CLSM and exposed to a chloride solution or distilled water environment. The center of the metallic coupon was placed at the center of the cylinder, 50 mm from the top surface. Because CLSM is a low strength material, care was taken not to damage the samples after casting. Precutting the plastic cylinders longitudinally and taping these cuts closed prior to casting minimized damage for the uncoupled specimens. After curing, the plastic cylinder was separated from the CLSM to allow for the direct exposure of the CLSM to the environment. The CLSM cylinders were not removed from the plastic cylinders in order to prevent possible damage to the low strength CLSM samples.

To evaluate the impact of embedding ductile iron and galvanized steel in different environments (coupled state) on the corrosion performance of these materials, metallic coupons were embedded in 100 x 200 mm plastic cylinders as shown in Figure 4b. Note that one metallic coupon was completely embedded in the CLSM and the other coupon was completely embedded in the soil. These coupons were electrically coupled with a 10 Ohm resistor soldered to the top of the connector rods. To cast a coupled sample, the cylinder was laid on its side. A 38 x 100 mm plexiglass sheet was glued to the top of the cylinder, covering one-half of the top opening. Three-millimeter diameter threaded connector rod, connected to the metallic coupon, was attached to the plexiglass with one nut on each side of the plexiglass to secure the rod in place. The hole in the plexiglass was drilled such that the coupon would have 5 mm of CLSM cover (i.e., offset 7 mm from the center of the cylinder) when the sample was cast on its side. The top of the metallic coupon was embedded to a depth 98 mm below the top of the cylinder. After the metallic coupon was secured, the CLSM was placed in the cylinder lying on its side. The sample was then covered with wet burlap for 1 day and then cured. After curing, sand or clay was placed in three equal layers and compacted in the remaining cylinder not filled with CLSM. A metallic coupon was placed opposite the coupon embedded in the CLSM, 5 mm from the face of the CLSM. Six holes (4 mm diameter) were drilled at 15 mm above the bottom of each cylinder and the holes were wrapped with a filter paper that would allow the chloride solution or distilled water to enter into the cylinders but would prevent the soils from being washed out of the cylinders.

Control samples were similar to the uncoupled samples, but metallic coupons were completely embedded in sand.

Ductile iron coupons, 13x24x4 mm in size, were machined from a 300 mm diameter commercially available ductile iron pipe (AWWA C151, Grade 60-42-10) and zinc galvanized steel coupons, 13x24x3.5 mm in size, were machined from a 300 mm diameter zinc galvanized steel culvert (uncoated thickness approximately 3.40 mm). To better represent the actual corrosion performance of the pipe material, care was taken during the sample fabrication to minimize damage to the "as received" mill scale on the samples. The cut edges were coated with low viscosity, two part epoxy to prevent corrosion on the edges.

All samples were covered with wet burlap for 1 day after casting and then cured for 27 days following ASTM C192/C192M-02, *Standard Practice for Making and Curing Concrete Test Specimens in the Laboratory*, in a curing room with a temperature of 23 ± 2°C and a relative humidity greater than 98%. Later samples were exposed to a 3.0% sodium chloride solution or distilled water. The liquid level was maintained at a level of 90 mm throughout the test program.

Experimental Design

The laboratory study was performed in two phases. In the first phase study more CLSM samples were evaluated with lower number of samples and in the second phase a lower number of CLSM mixtures were evaluated with higher number of samples for a better statistical analysis. Both in phase I and II, uncoupled and coupled samples were prepared and tested.

Phase I Investigation

The influences of thirty different CLSM mixtures and one sand type (control sample) on the corrosion performance of metals were evaluated. The mixture proportions and fresh CLSM characteristics are shown in Table 2. Eight mixtures were duplicated to evaluate the repeatability of the test results. Repeated mixtures are identified with an "R" next to their mixture number. A liquid air entraining agent (AEA) specifically designed for CLSM was used in mixtures 16 through 23 and mixture 26. Mixtures 26, 27, and 28 contained a liquid, non-chloride accelerating admixture meeting ASTM C494, *Standard Specification for Chemical Admixtures for Concrete*, Type C requirements. In the first phase study only ductile iron coupons were evaluated. Three coupled and uncoupled samples for each of the thirty-eight CLSM mixtures and five control samples were fabricated. All of the samples were exposed to 3.0% sodium chloride solution for 18 months. The control samples and the soil section of coupled samples were filled with a sand meeting the "graded sand" requirements of ASTM C778, *Standard Specification for Standard Sand*.

Table 2 Phase I CLSM mixture proportions and fresh characteristics.

Mix No	**Cement Content (kg/m^3)**	**Fly Ash Type**	**Fly Ash content (kg/m^3)**	**Fine Aggregate Type**	**Water Demand (kg/m^3)**	**Flow (mm)**	**Total Bleeding (%)**	**Air Content (%)**	**Fresh Unit Weight (kg/m^3)**
1	30	Class C	180	CS	211	200	-	0.9	1965
1R	30	Class C	180	CS	206	210	2.08	0.9	1974
2	60	Class C	180	CS	206	200	2.45	0.95	2108
2R	60	Class C	180	CS	206	250	0.21	0.5	2291
3	60	Class C	360	BA	577	180	4.32	1.65	1754
3R	60	Class C	360	BA	541	200	2.58	2.1	1997
4	30	Class F	360	CS	220	200	0.39	2.2	2199
4R	30	Class F	360	CS	220	220	2.92	1.8	2211
5	60	Class F	180	BA	600	180	5.84	2.5	1739
5R	60	Class F	180	BA	600	160	7.2	1.4	1887
6	30	HC	360	CS	315	200	2.26	1.3	2103
7	30	Class F	180	FS	501	200	0.57	2.1	1817
8	60	HC	180	FS	532	240	1.04	3.3	1647
9	60	Class F	360	FS	520	200	0.54	2.5	1684
10	30	HC	180	BA	628	140	4.81	2	1681
11	60	HC	360	BA	573	230	6.42	1.7	1743
12	30	Class C	360	BA	572	220	3.64	2.7	1774
13	60	Class C	360	FS	499	200	0	1.8	1902
14	60	Class F	360	CS	216	220	1	1.3	2174
15	30	Class C	360	FS	486	200	0.13	2.75	1741
16	30	None	0	CS	295	200	2.33	16	1922
16R	30	None	0	CS	295	190	2.35	15.5	1874
17	30	None	0	BA	582	130	4.35	20	1447
18	60	None	0	CS	200	220	0.7	16.5	1836
19	30	None	0	BA	492	130	1.08	25	1385
20	60	None	0	BA	525	130	3.41	18.5	1485
20R	60	None	0	BA	525	130	1.44	15.5	1511
21	30	None	0	CS	170	180	0.62	25.5	1789
22	60	None	0	CS	131	200	0.05	26.5	1748
22R	60	None	0	CS	136	180	0.43	25.5	1802
23	60	None	0	BA	454	140	1.3	28.5	1382
24	60	Class F	1200	None	486	240	2.25	2.8	1635
25	60	HC	1200	None	853	240	7.38	1.3	1322
26	60	None	0	CS	136	170	0	25.5	1802
27	60	Class F	1200	None	486	230	1.28	0.7	1638
28	60	Class F	180	CS	220	200	1.33	1.4	2182
29	60	None	0	FS	373	230	0.28	2.6	1812
30	30	None	0	FS	414	200	0.4	2	1789

CS – concrete sand
BA – bottom ash
FS – foundry sand
HC – high carbon

Phase II Investigation

Thirteen CLSM mixtures were cast to evaluate the corrosion of metals embedded in CLSM. The proportions of CLSM mixtures and their unit weights are shown in Table 3. Small case letters added to the mixture names indicate separate batches. The corrosion performance of ductile iron and galvanized steel coupons were evaluated. A minimum of five coupled and five uncoupled samples were prepared for each of the thirteen CLSM mixtures. Totally, over 1000 samples were evaluated in the second phase study. Half of the samples were exposed to 3.0% sodium chloride solution and the rest were exposed to distilled water for 26 months. One of the two types of soils (sand and clay) was used to fill the soil section of each coupled sample. The sand met the "graded sand" requirements of ASTM C778. The clay used was obtained from the National Geotechnical Experimentation Site located on the Texas A&M University Riverside Campus. The plastic and liquid limits of the clay were 20.9% and 53.7%, respectively, and the hydraulic conductivity coefficient was measured as $5x10^4$ m/yr.

The CLSM mixtures used in the research program contained portland cement, fly ash, water, and fine aggregates. The materials and the mixture proportions selected for this study were based on a survey of current practice; in addition, experimental design software was used to select the actual mixtures from a range of possible mixtures to allow for subsequent interpolation and extrapolation of research findings (Folliard et al. 1999). Mixtures differed in the quantity of cement, the type of fine aggregate, and the type and quantity of fly ash used. Water was added to each mixture to achieve a flow of approximately 200 mm. Flow was measured following ASTM D 6103-97, *Standard Test Method for Flow Consistency of Controlled Low Strength Material (CLSM)*.

ASTM Type I cement was used for all the mixtures. The chemical composition of the cement used in the research is shown in Table 4.

Three fly ashes were included in the study, including one Class C and one Class F fly ash (based on ASTM C 618, *Standard Specification for Coal Fly Ash and Raw or Calcined Natural Pozzolan for Use as a Mineral Admixture in Concrete*). The third fly ash had a loss-on-ignition (LOI) value of over 14 percent and is referred throughout this paper as a "high-carbon" fly ash. The high-carbon ash exceeds the 6 percent maximum LOI value specified in ASTM C 618. The chemical compositions and LOI values of the fly ashes and foundry sand used in the research are shown in Table 5. High-carbon off-spec fly ashes are often not used in conventional concrete because they increase the water requirement and admixture dosage, especially air-entraining agent dosage. However, these ashes are acceptable and widely used for CLSM, which is desirable as a low strength material.

Table 3 CLSM mixture proportions and unit weights.

Mix	Cement Content (kg/m^3)	Fine Aggregate Content (kg/m^3)	Fine Aggregate	Fly Ash Content (kg/m^3)	Fly Ash Type	Water Content (kg/m^3)	Flow (mm)	Air Content (%)	Unit Weight (kg/m^3)
A1a	63	0	None	1200	F	184	209	1.5	1605
A1b	63	0	None	1200	F	432	203	1.3	1591
A1c	63	0	None	1200	F	515	200	1	1605
A2a	0	1500	CS	206	C	134	200	1.5	2177
A2b	0	1500	CS	206	C	200	305	0.6	2180
A3a	30	1500	CS	0	None	98	178	30	1602
A3b	30	1500	CS	0	None	118	200	25	1695
A3c	30	1500	CS	0	None	111.7	200	29	1593
A4a	15	1500	CS	180	F	190	216	1.5	2194
A4b	15	1500	CS	180	F	204	229	1.3	2169
A4c	15	1500	CS	180	F	196	216	1.5	2167
A5a	30	1500	CS	180	F	184	203	2	2185
A5b	30	1500	CS	180	F	188	203	2.3	2163
A5c	30	1500	CS	180	F	170	225	1	2177
A6a	15	1500	CS	180	HC	190	210	2	2115
A6b	15	1500	CS	180	HC	224	203	2	2097
A6c	15	1500	CS	180	HC	216	206	1	2084
A7a	30	1500	CS	180	HC	232	203	2.3	2099
A7b	30	1500	CS	180	HC	232	203	1.3	2111
A7c	30	1500	CS	180	HC	214	206	1.8	1978
A8a	15	1500	CS	180	C	168	216	4.8	2155
A8b	15	1500	CS	180	C	168	216	1.8	2220
A8c	15	1500	CS	180	C	174.4	200	1.5	2179
B10a	30	1500	BA	180	C	318	175	1.5	1852
B10b	30	1500	BA	180	C	318	200	2	1848
B4a	30	1500	CS	180	C	186	216	4.8	2170
B4b	30	1500	CS	180	C	144	216	1.3	2225
B4c	30	1500	CS	180	C	184	200	1.8	2228
B6a	30	1500	CS	180	HC	472	209	2.3	1753
B6b	30	1500	FS	180	HC	494	203	1.8	1765
B6c	30	1500	FS	180	HC	524	200	1.5	1750
B7a	30	1500	FS	180	C	484	222	1.5	1795
B7b	30	1500	FS	180	C	426	229	3	1848
B9a	15	1500	BA	180	HC	324	165	1.8	1821
B9b	30	1500	BA	180	HC	324	145	2.8	1760

CS - concrete sand; BA - bottom ash; FS - foundry sand; HC - high carbon; “-” indicates data not obtained.

Note 1: All CLSM mixtures containing fine aggregate had 1500 kg/m^3 of fine aggregate.

Note 2: Because flow was the key parameter and the amount of water influenced the amount of flow, all mixtures volumes may not be exactly 1 m^3.

Table 4 Chemical composition of Type 1 portland cement.

Chemical compound	% by weight
Silicon Dioxide, SiO_2	21.0
Aluminum Oxide, Al_2O_3	4.9
Iron Oxide, Fe_2O_3	2.3
Calcium Oxide, CaO	64.8
Magnesium Oxide, MgO	1.7
Sodium Oxide, Na_2O	0.3
Compound composition	
C_3S	62.0
C_2S	13.0
C_3A	9.0
C_4AF	7.0

Table 5 Chemical composition of fly ashes and foundry sand.

Chemical compound	Percent by weight			
	Class F Fly Ash	Class C Fly Ash	High-Carbon Fly Ash	Foundry Sand
Silicon Dioxide, SiO_2	55.24	34.40	47.29	85.20
Aluminum Oxide, Al_2O_3	29.43	20.20	19.53	3.92
Iron Oxide, Fe_2O_3	5.19	5.76	5.21	3.46
Total (SiO_2+ Al_2O_3+ Fe_2O_3)	89.86	60.36	72.03	92.58
Calcium Oxide, CaO	1.59	26.73	6.01	0.79
Magnesium Oxide, MgO	0.93	5.15	2.05	0.58
Sodium Oxide, Na_2O	0.24	1.58	2.47	0.98
Potassium Oxide, K_2O	2.18	0.36	0.83	0.17
Titanium Dioxide, TiO_2	1.44	1.32	0.75	0.21
Manganese Dioxide, MnO_2	0.03	0.06	0.04	0.11
Phosphorus Pentoxide, P_2O_5	0.28	1.08	0.40	0.00
Strontium Oxide, SrO	0.10	0.39	0.31	0.01
Barium Oxide, BaO	0.07	0.60	0.30	0.07
Sulfur Trioxide, SO_3	0.38	1.98	0.38	0.20
Loss on Ignition (LOI)	2.90	0.37	14.44	
Specific Gravity	2.41	2.51	2.09	

Concrete sand, bottom ash, and foundry sand were used as fine aggregates. Fine aggregate gradations were determined following ASTM C 136, *Standard Test Method for Sieve Analysis of Fine and Coarse Aggregates*. The bottom ash was slightly coarser and the foundry sand was finer than the limits imposed by ASTM C 33, *Standard Specification for Concrete Aggregates*. The absorption capacities and specific gravities of the constituent materials were determined following ASTM C 128, *Standard Test*

Method for Density, Relative Density (Specific Gravity), and Absorption of Fine Aggregate. The chemical composition of the foundry sand was shown in Table 5. The absorption capacities, specific gravities, and fineness modulus of fine aggregates are shown in Table 6.

Table 6 Material characteristics of fine aggregates.

Material	Type	Specific Gravity	Absorption (%)	Fineness Modulus
Fine Aggregate	Concrete Sand	2.60	1.00	3.00
	Foundry Sand	2.36	5.60	2.14
	Bottom Ash	2.28	8.90	2.89

In both phases, metallic coupons were removed from the samples at the end of the exposure period and were evaluated for mass loss following ASTM G1, *Standard Practice for Preparing, Cleaning, and Evaluating Corrosion Test Specimens.* Ductile iron coupons were cleaned using cleaning procedure C.3.5 and galvanized steel coupons were cleaned using cleaning procedure C.9.5. In the case of coupled samples, only the coupons embedded in the sand were evaluated for mass loss as it was determined early in this study that this would be the anode. The coupon embedded in the CLSM on these samples exhibited limited corrosion, if any. Evaluation of the coupons was based on the amount of mass loss resulting from corrosion divided by the original mass of coupons resulting in percent mass loss values.

In the first phase study, the resistivity of the CLSM and sand were evaluated using a resistivity box (or soil box) as described in ASTM G57, *Standard Test Method for Field Measurement of Soil Resistivity Using the Wenner Four-Electrode Method*. Resistivity measurements were obtained from saturated samples at 182 days after casting. These samples were cast at the same time with the corrosion samples (i.e., the CLSM came from the same batch for both sample types). In the second phase study, the resistivity of CLSM and soils were not measured from separately cast samples, but from each of the actual exposed uncoupled and coupled samples following ASTM G57. Four stainless steel pins were used as electrodes instead of a soil box with a soil resistance meter to measure the resistance of cylindrical CLSM samples as shown in Figure 5. The electrodes were placed at an equal distant of 25.4 mm from each other, measuring the resistance of CLSM at a depth of 25.4 mm. The results of the first phase study indicated that resistivity was not a significant factor, however resistivity was found to be a significant factor in the second phase study.

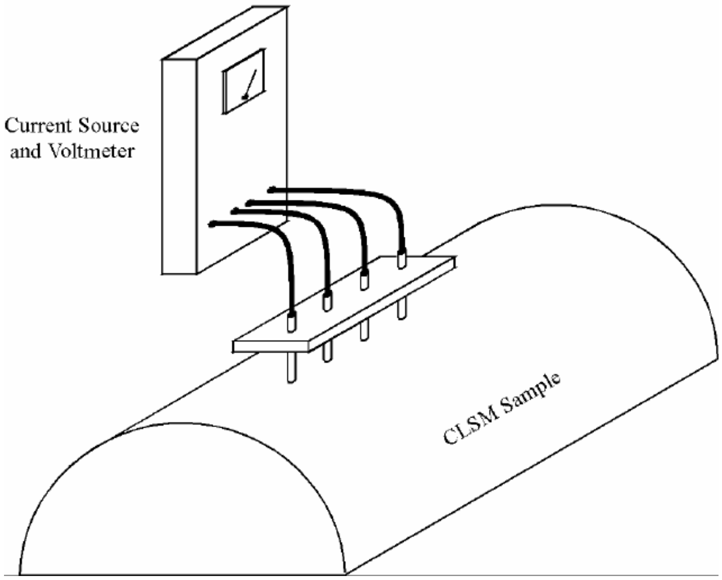

Figure 5 Resistivity measurement with Wenner Four-Electrode Method.

The difference in measurement techniques is believed to be the reason for the different results obtained in the statistical analysis. The resistivity measured from a separate sample cast in a soil box could be a better indicator of the inherent resistivity property of the CLSM mixture. However, the actual resistivity of the CLSM in exposed conditions will depend on many factors such as soluble salt concentration and the saturation level. The finding of this study that resistivity is a statistically significant factor, indicates that the mass loss data of coupons was better correlated to the actual resistivity values measured from the exposed samples. Edgar also found that the corrosion of galvanized culverts in the field were much better correlated to the field resistivity measurements than the saturated soil resistivity measurements using a soil box (Edgar 1989). He suggested that the difference in correlations could be due to the different saturation levels of the soil box testing and the field conditions throughout the service life of the pipes.

In the first phase study two 50 x 100 mm cylinders were cast for each CLSM mixture at the same time as the corrosion samples were cast to evaluate their pH. At 182 days after casting, the CLSM cylinders were removed from the curing room and their pore water solution was immediately evaluated for pH. In the second phase study, 1:1 by weight of CLSM and distilled water solutions were prepared from each exposed uncoupled and coupled sample to evaluate for pH. In both phases, a pH combination electrode connected to a benchtop multimeter with a precision of 0.01 was used to measure pH. In the second phase, the pH of soil samples used in the coupled samples was also determined using 1:1 by weight distilled water solutions. Because only one type of clay and only one type of sand was used in the samples, only randomly selected soil samples from coupled samples exposed to the chloride and distilled water environments were collected and tested. One soil pH value was determined for each type of soil exposed to each type of environment in a coupled sample.

In the second phase also a test method developed under the Strategic Highway Research Program to rapidly determine the chloride content of mortars and concrete was used to determine the chloride content of the CLSM and soil samples that were exposed to the chloride solution (Cady and Gannon 1992).

Results and Statistical Analysis

The results and the statistical Analysis of the uncoupled and coupled samples of the two phases are provided in four separate sections.

1. Phase I – Uncoupled Samples

The resistivity and pH values for the CLSM mixtures are shown in Table 7. The box plot showing the distribution of the average percent mass loss values of the ductile iron samples is given in Figure 6. It can be seen that samples 21 and 23 are extreme outliers, i.e., the difference between the 75th quartile of the data and these samples is larger than three times the range of the data. Because these mixtures are not significantly different from the others and these results seem to be an anomaly, these data will not be included in the statistical analysis.

Table 7 Phase I resistivity and pH of CLSM mixtures.

Mixture No.	pH @ 182 days	Resistivity (ohm-cm) @ 182 days	Mixture No.	pH @ 182 days	Resistivity (ohm-cm) @ 182 days
1	11.4	2593	15	8.63	2122
1R	10.33	3484	16	11.32	1834
2	9.8	2855	16R	9.8	2881
2R	11.9	3882	17	11.01	2310
3	11.65	2698	18	11.93	4128
3R	11.58	3248	19	12.64	7072
4	11.12	--	20	12.89	5291
4R	11.2	8487	20R	12.97	8644
5	11.24	--	21	12.53	7387
5R	12.25	12,573	22	12.3	8120
6	8.7	10,478	22R	12.3	3824
7	10.8	3196	23	11.4	3536
8	11.18	3222	24	11.53	1582
9	11.1	1441	25	12.93	1048
10	11.28	1781	26	9.07	3091
11	11.3	3468	27	13.03	3065
12	11.58	4086	28	12.65	6287
13	10.1	5605	29	11.28	3143
14	11.4	12,049	30	11.2	1624

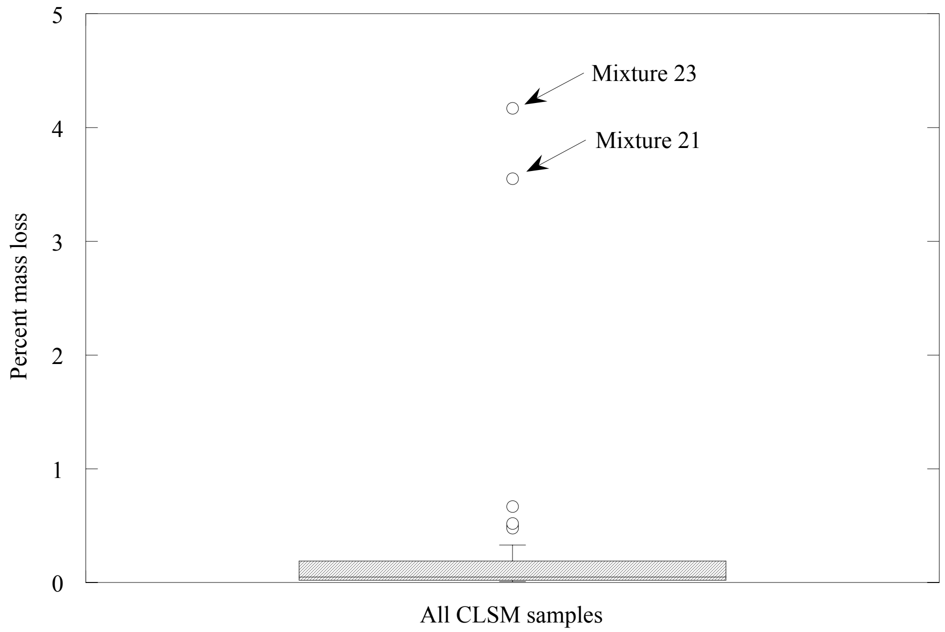

Figure 6 Phase I percent mass loss of ductile iron coupons embedded in all CLSM types.

A multiple regression and analysis of variance was performed with the average percent mass loss data of the thirty-six CLSM samples as the response variable. However, the data was transformed by taking the logarithm of the data. Cement content, fine aggregate type, fly ash type, resistivity, pH, and water-cementitious materials ratio (w/cm) were taken as the explanatory variables. The first model used to evaluate the results only considered the main effects, i.e., interactions between the explanatory variables were initially assumed to be negligible. The p-value for the overall model was 0.0002 and the coefficient of multiple determination (R^2) was 0.76, i.e., 76% of the observed variation in the data is attributable to variation among predictions based on the fitted model. The probability of occurrence of such a proportion is less than 1% if there is no relation between the response variable and the explanatory variables. Thus, there is strong statistical evidence that the logarithm of the percent mass loss data is related to the explanatory variables in the model. However, the significance analyses of the estimated explanatory variable coefficients show that only the coefficients for the fly ash type and fine aggregate type are significant at the 90% confidence level.

Comparison of all possible main effect models for the maximum adjusted R^2 and minimum mean sum of error (MSE) indicates that the best model to predict mass loss of ductile iron pipe completely embedded in CLSM has three explanatory variables; fly ash type, fine aggregate type, and w/cm as shown below:

$$\log_{10}(\%\,mass\,loss) = 0.056 - \gamma - \lambda + 0.0312 \cdot \frac{w}{cm} \qquad (1)$$

where, γ is 1.13, 1.068, 1.313, and 0.0 are for bottom ash, concrete sand, foundry sand, and no fine aggregate, respectively, and λ is 0.467, 0.614, 0.688, and 0.0 for Class C, Class F, high-carbon, and no fly ash, respectively. The logarithm of the percent mass loss data is the response variable. The adjusted R^2 for this second model is 67% and its

MSE is 0.0916. Appropriate coefficients should be used to predict the percent mass loss of a specific mixture.

Figure 7 shows the observed values against the predicted percent mass loss values obtained from the second model. The analysis also indicates that there are no outliers in the data (except mixtures 21 and 23 removed earlier) and the residual plot showed that residuals are independent of the values of the predictor variables. There are no influential observations, i.e., there are no data points that solely have a large impact on model properties. The coefficients for the fine aggregate type and the fly ash type are significant at the 95% confidence level and the coefficient for the w/cm is significant at the 89% confidence level.

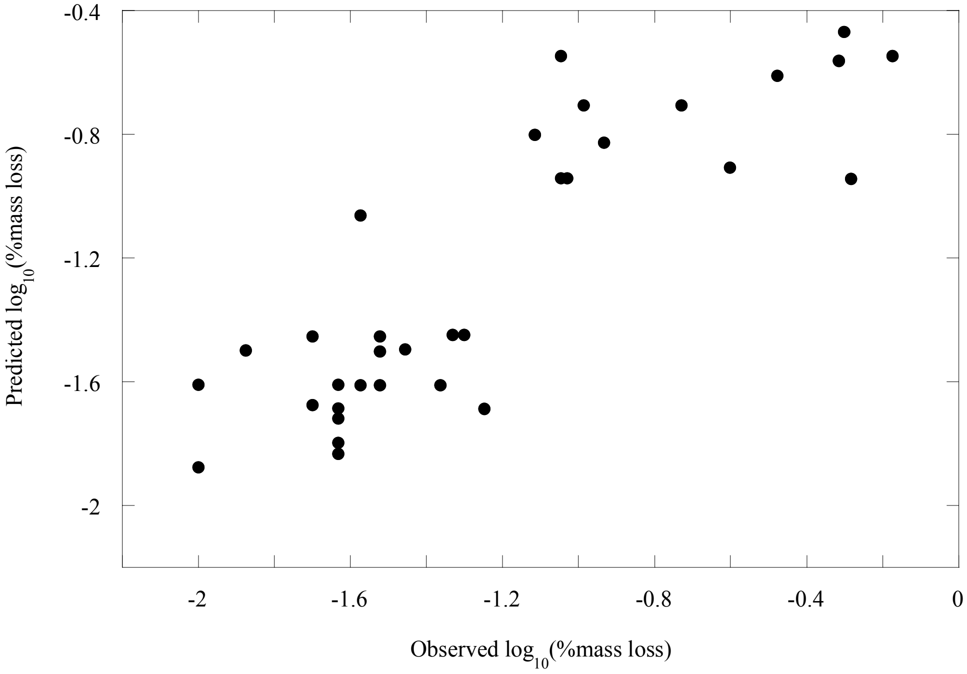

Figure 7 Predicted versus observed mass losses for three explanatory variables; fly ash type, fine aggregate type, and w/cm.

Percent Mass Loss versus Resistivity

Many field investigations on the corrosion of metals embedded in soils have reported that resistivity is a major controlling parameter affecting corrosion activity of the embedded metal (Spickelmire 2002, Kozhushner et. al. 2001). An exception to this is when severe microbiological activity is present (Palmer 1989). Figure 8 compares the mean percent mass loss of the coupons embedded in the thirty-six different CLSM mixtures with the resistivity of the CLSM mixtures measured at 182 days. Prior corrosion research in soils reported non-linear relationships between mass loss and resistivity (Edgar 1989, Palmer 1989) as follows:

$$Mass\ Loss = \alpha \cdot r^{-\beta} \tag{2}$$

where r is the resistivity (Ω-cm) and α and β are constants. However, the evidence for such a non-linear relationship for the CLSM data shown in Figure 8 is very weak.

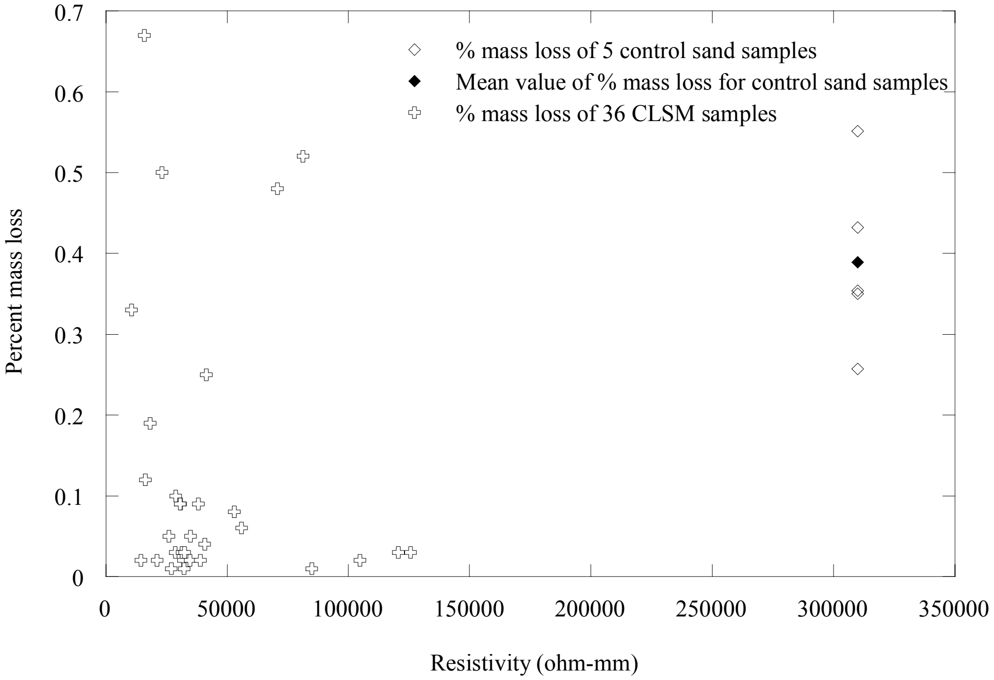

Figure 8 Percent mass loss values versus resistivity.

Figure 8 also shows the percent mass loss values of the control group (i.e., the ductile iron samples embedded in standard sand). The average percent mass loss for the control group was 0.39%. The control sand exhibited a resistivity of $3.1\text{x}10^4$ Ω-cm. Ductile iron pipe embedded entirely in CLSM exhibited lower corrosion activity than the ductile iron samples embedded in the control sand even though the resistivity of the control sand material was higher than the resistivity of all the CLSM mixtures. Although it is reported throughout the literature that corrosion rates are inversely proportional to the material resistivity, resistivity alone may not be a reliable indicator of corrosion potential for ductile iron pipes embedded in CLSM. These results agree with earlier research by Abelleira et al. (1998), which reported that resistivity is not a good measure of the potential corrosivity for CLSM.

The non-linear relationship shown in equation 2 implies a linear relationship between the natural logarithm of the mass loss and the natural logarithm of resistivity.

$$\ln(\mathit{Mass\ Loss}) = \ln(\alpha) - \beta \ln(r) \tag{3}$$

The correlation coefficient (R) between the natural logarithm of percent mass loss of the coupons embedded in CLSM and the natural logarithm of resistivity values is only 0.084 and α and β are 0.87 and 0.21, respectively.

It should be noted that in phase I the resistivity of the CLSM was measured on samples exposed to standard curing conditions. The resistivity of these samples may not represent the actual in place resistivity of the exposed samples. In Phase 2 of this research program, the resistivity was measured from the actual exposed samples.

Percent Mass Loss versus Fly Ash Type

Some utility agencies have voiced concern regarding the use of fly ash in CLSM and how it influences the corrosion performance of their pipes. In some cases, utility agencies do not allow the use of fly ash in CLSM, even though there have been no documented studies addressing the influence of fly ash in CLSM on the corrosion performance. Thus, there is a need to document the corrosion performance of pipes embedded in CLSM containing fly ash.

It has been well established that SCMs react with calcium hydroxide to form calcium silicate hydrates. This delayed reaction between the siliceous mineral admixture and the calcium hydroxide consumes the calcium hydroxide, resulting in a reduction of the pH pore solution (Diamond 1981, Holden 1983). Because a reduction in the pH could result in higher corrosion activity, fly ash may be detrimental to the corrosion performance of pipe embedded in CLSM containing fly ash. Byfors (1987) reported that the addition of 40% fly ash to a concrete mixture resulted in the reduction in the pore solution pH, which reduced the chloride threshold level to approximately half of that of the corresponding mixture without fly ash. But, the addition of fly ash to a cement-based system also results in a refined pore structure and typically, reductions in the diffusivity, permeability, and porosity. Cao et al. (1994) reported that fly ash blended cement pastes showed superior passivation characteristics over longer-terms.

Figure 9 compares the pH values of CLSM samples with and without fly ash. Tukey's comparison at a 90% level indicates that there is no statistical evidence of a difference among true pH means of the different fly ash types.

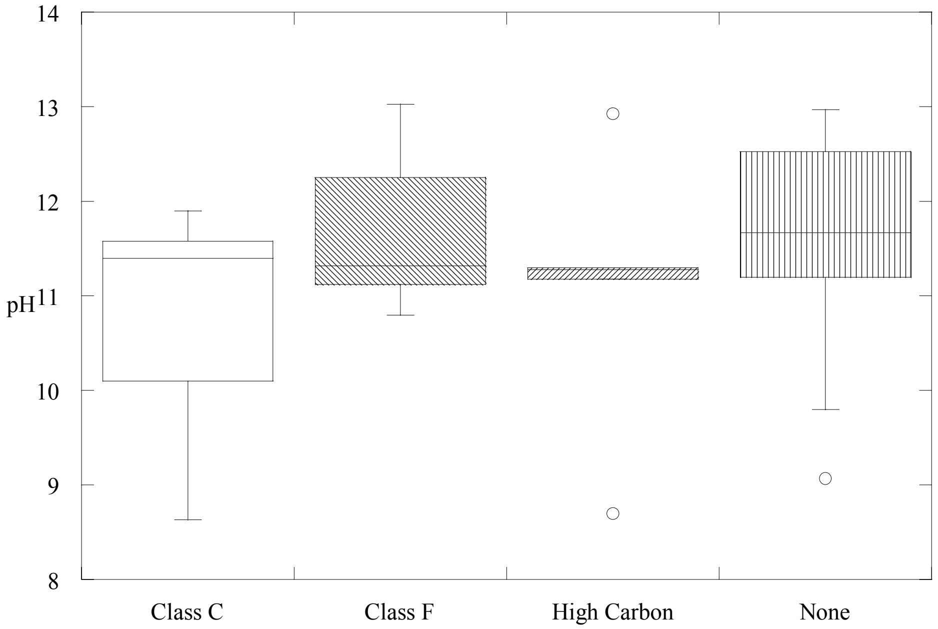

Figure 9 Distribution of pH of pore solution values for CLSM mixtures with different types of fly ashes.

Figure 10 shows the influence of fly ash type on logarithm of the mass loss of the ductile iron pipe embedded in the various CLSM mixtures. The figure shows that the addition of fly ash reduces the logarithm of the percent mass loss of the ductile iron samples resulting from chloride-induced corrosion. Statistically, there is no significant difference at the 95% confidence level between the logarithm of the mean percent mass losses of the coupons embedded in the CLSM mixtures containing class C, class F, and high carbon fly ashes. However, the logarithm of the mean percent mass loss of mixtures without fly ash is statistically significantly higher than the mixtures with fly ash. This indicates that the benefits of the fly ash on the microstructure and long-term passivation characteristics, as reported by Cao et al. (1994), likely has a more significant impact on corrosion performance than the relatively limited reduction in pH.

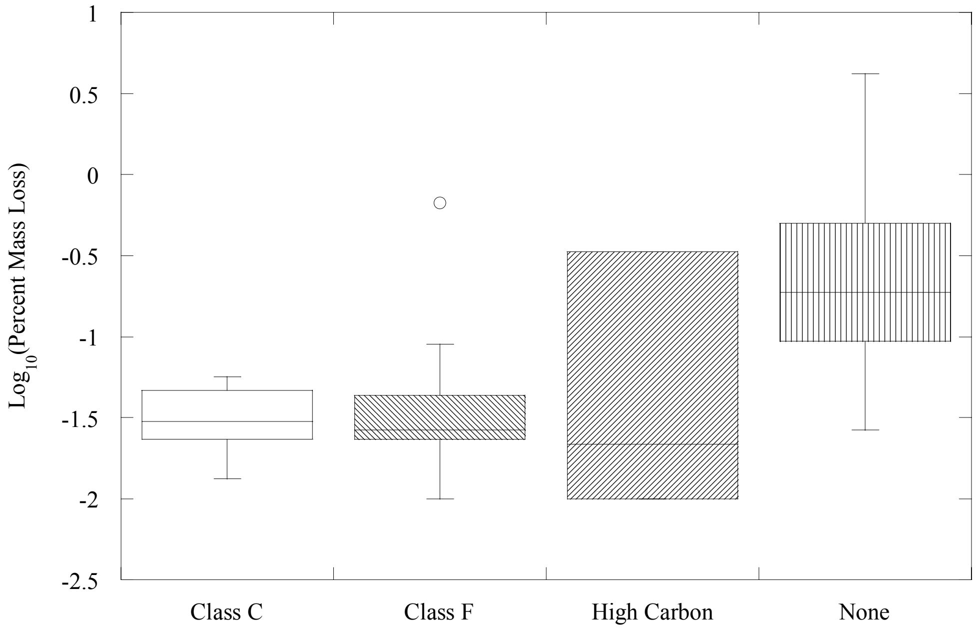

Figure 10 Distribution of percent mass loss values for coupons embedded in CLSM with different types of fly ash.

Percent Mass Loss versus pH

The hydration process of cementitious materials results in a high pH pore water solution. It has been well established that this high pH solution results in the formation of a passive, protective film on the surface of steel (Broomfield 1997). From Table 7, it can be seen that the pH of the CLSM mixtures is generally higher than 10. The mean pH of the pore solution from the CLSM mixtures evaluated in this study was 11.35. The pH of the control sand pore solution used in this study was 7.46. Because the pH of the CLSM pore solution is higher than the pH of the control sand pore solution, it would be expected that the CLSM would provide more protection against corrosion than the control sand.

Figure 11 shows the mass loss as a function of pH for both the samples embedded in CLSM and in the control sand material. Although pH is expected to decrease the corrosion performance of the ductile iron pipe, the results do not indicate a significant decrease in the percent mass loss as a result of the increased pH. As such, the pH of the pore solution alone does not seem to reliably estimate the corrosion performance of ductile iron pipe embedded in CLSM. Prior research in soils has also stated that in most cases pH is only significant in distinguishing between otherwise similar soils (Palmer 1989).

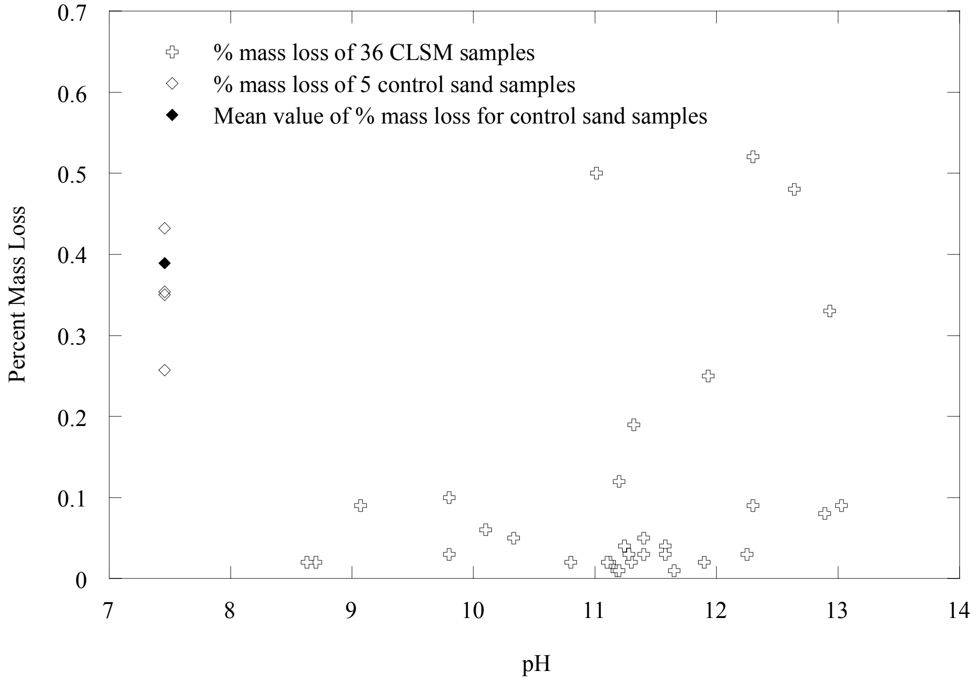

Figure 11 Percent mass loss from corrosion as a function of pore solution pH.

Percent Mass Loss versus Aggregate Type

A wide selection of materials can be used in CLSM as fine aggregates. CLSM producers have successfully used many locally available materials; however, conventional concrete sand is the most commonly used aggregate (Folliard et al. 1999). Foundry sand is another material used successfully in CLSM (Bhat and Lovell 1997, Stern 1995). The Federal Highway Administration (FHWA) issued a report that covers in detail the use of foundry sand in CLSM (FHWA 1998). The Environmental Protection Agency (EPA) has also recognized foundry sand as a suitable material for CLSM (EPA 1998). Bottom ash, a by-product of coal combustion, has also been successfully used in CLSM (Naik et al. 1998).

A statistical analysis of the data obtained in this study indicates that the fine aggregate type used in a CLSM mixture has a significant effect on the percent mass loss data. Figure 12 shows the logarithm of the percent mass loss distribution by fine aggregate type. Tukey’s comparison at a 95% confidence level indicates that the mean logarithm of percent mass loss data for mixtures containing bottom ash, concrete sand, and foundry sand are statistically not different from each other. However, the mean logarithm of percent mass loss data for the coupons embedded in mixtures without fine aggregates is statistically different and higher than the other mixtures containing fine aggregate.

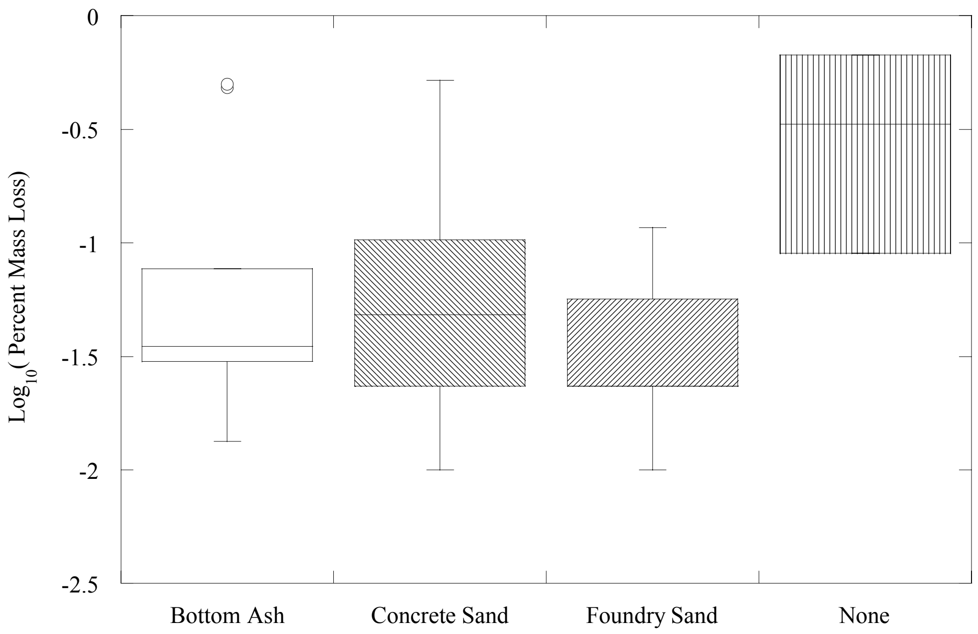

Figure 12 Logarithm of mass loss versus aggregate type.

Previous research on pore structures of mortars has shown that increasing fine aggregate volume concentration caused the porosity of mortar specimens to decrease linearly while increasing their density for all curing periods up to 6 months (Okpala 1989). Following the same logic, the decrease in percent mass loss could be due to reductions in the diffusivity, permeability, and/or porosity of the CLSM mixtures containing fine aggregates. This study indicates that as long as CLSM contains a fine aggregate the percent mass loss of the embedded pipe will be lower when compared with CLSM mixtures containing no fine aggregates.

Percent Mass Loss versus Cement Content

The amount of cement used in CLSM mixtures is very low compared to the amount of water used. The statistical analysis indicates that the cement content had no significant effect on the percent mass loss of the ductile iron coupons embedded in the CLSM mixtures. However, the ratio of the amount of water to the amount of cement together with fly ash had a more significant effect on the percent mass loss data.

Percent Mass Loss versus w/cm

For conventional concrete, it has been well established that as the w/cm decreases (within reason), the strength increases and the diffusivity, porosity, and permeability decreases. Other characteristics are also improved. Thus, for uncracked concrete, as the w/cm ratio is decreased, corrosion of embedded steel would be reduced due to the improved concrete characteristics. For CLSM, the w/cm is typically very high. The influence of w/cm for CLSM mixtures on the corrosion performance of ductile iron pipe has not been reported. Figure 13 shows the logarithm of the percent mass loss of the ductile iron pipe embedded in the CLSM as a function of the w/cm of the CLSM mixtures containing fly ash and fine aggregates. As with the other plots of mass loss, the outliers are not included in the analysis. It can be seen that the percent mass loss slightly increases with increasing w/cm.

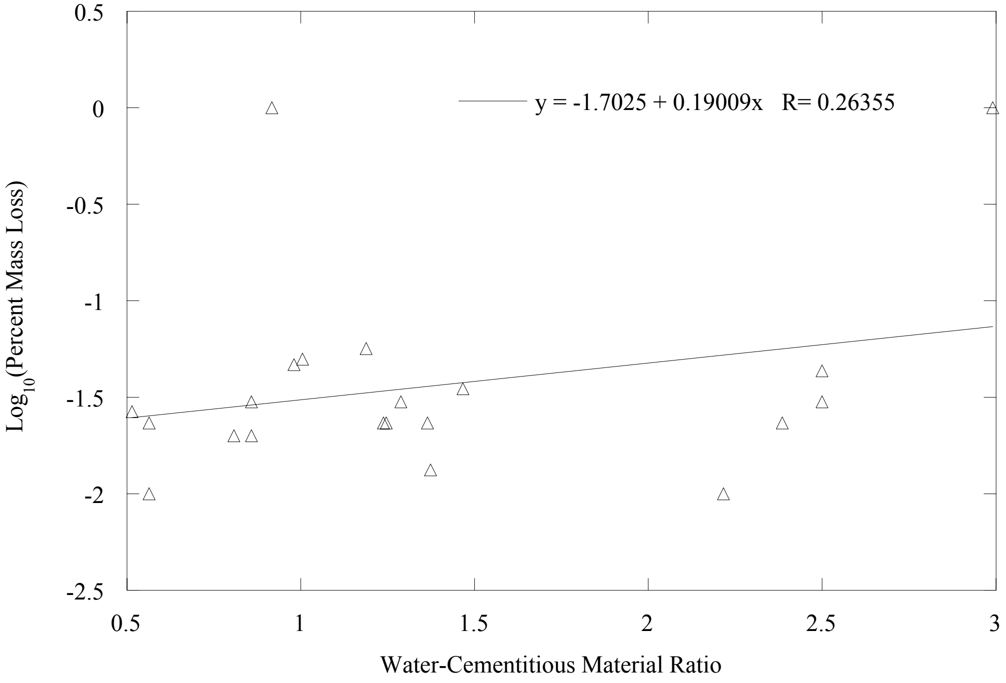

Figure 13 Percent mass loss versus w/cm.

2. Phase I – Coupled Samples

To evaluate the mass loss (i.e., corrosion performance) of the coupled ductile iron coupons embedded in both CLSM and sand, a similar statistical analysis as described in phase I – Uncoupled samples was performed. The effects of cement content, fine aggregate type, fly ash type, resistivity, pH, and water-cementitious materials ratio (i.e., the explanatory variables) on the average percent mass loss of the ductile iron specimens embedded in sand were evaluated. The average percent mass loss (i.e., the response variable) was transformed by taking its logarithm. Figure 14 shows the histogram of the transformed percent mass loss values for the ductile iron coupons embedded in the sand of the galvanically coupled samples after the transformation. The p-value for the normality test after the transformation was 0.83, indicating a high likelihood of this distribution being normal.

An initial model for predicting percent mass loss was developed and used in the multiple regression analysis only considered the main effects of the explanatory variables, i.e., the interactions between the explanatory variables were assumed to be negligible. This initial model, considering all six explanatory variables, was determined to be statistically insignificant (as such it is not shown here). This indicated that the response variables alone, considering no interactions, used in this model could not explain the variance of the average percent mass loss values. Then models considering all possible interactions between the six explanatory variables were tested. Similar to the initial results, none of the models were statistically significant. These analyses indicated that a good prediction of percent mass loss using the explanatory variables was not possible for ductile iron pipe embedded in two different environments (i.e., galvanically coupled).

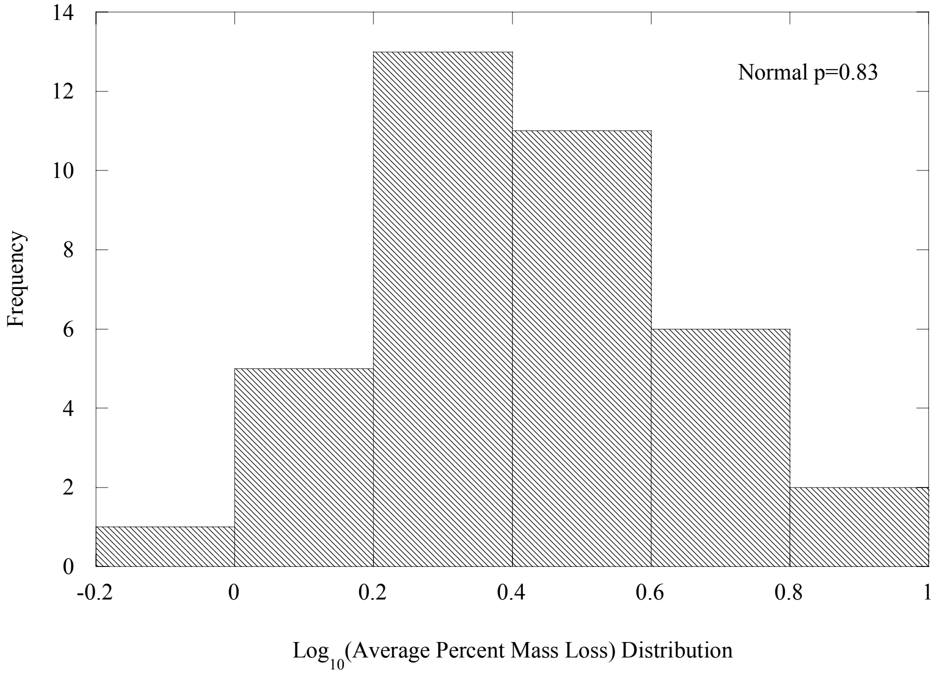

Figure 14 Histogram of the transformed percent mass loss of coupons embedded in sand section of coupled samples.

Examination of the percent mass loss values for the ductile iron specimens embedded solely in CLSM from the phase I – Uncoupled samples indicated that the percent mass loss values were related to three CLSM characteristics; fly ash type, fine aggregate type, and the water-cementitious materials ratio. These ductile iron specimens from the phase I – Uncoupled samples study likely corroded due to the formation of micro-galvanic corrosion cells on the surface of the single coupon because the anode and cathode were contained on a single coupon. These corrosion cells typically form due to differences of the metal surface or as a result of local differences in the CLSM environment directly adjacent to the ductile iron coupons. However, the major driving force of the corrosion of ductile iron specimens coupled in two different environments was likely a result of macro-galvanic corrosion cells formed due to the potential difference between the ductile iron specimens. Micro-galvanic cells likely had some effect on the corrosion, but it is believed that these effects were less significant when compared with the macro-galvanic effects. Because the sand and CLSM environments are significantly different, a corrosion potential difference sufficient to increase the corrosion activity was likely. For the phase I – coupled samples this potential difference had a much more significant impact on the corrosion performance than the cement content, fine aggregate type, fly ash type, resistivity, pH, and water-cementitious materials ratio of the CLSM mixtures.

Comparison of Phase I Coupled and Uncoupled Samples

The first part of the study found that there was a statistically significant difference in the percent mass loss of ductile iron coupons embedded in CLSM mixtures containing fly ash and fine aggregates when compared with CLSM mixtures not containing these materials. Figure 15 compares the logarithm of the distribution of percent mass loss of uncoupled samples (specimens embedded only in CLSM), coupled samples (specimens embedded in sand and connected to identical samples embedded in CLSM), and the control group (specimens embedded only in sand). The distributions are grouped by fly ash type. It can be seen that the coupling of the ductile iron coupons has a significant impact on the percent mass loss, whereas the effect of fly ash type was insignificant. Figure 16 shows the same comparison grouped by the fine aggregate type. As with the fly ash type, the effect of fine aggregate type is insignificant when compared with coupling of the ductile iron samples. Both figures indicate that the percent mass loss of ductile iron specimens embedded in sand and CLSM can be expected to be significantly larger than the specimens completely embedded in CLSM and the control group samples.

Embedding ductile iron pipes in different bedding or backfill materials could lead to higher corrosion activity, which is similar to the earlier research finding that soils with significantly different characteristics could also result in accelerated corrosion. However, because there is a significant reduction in corrosion activity for metallic pipe samples completely embedded in CLSM, with good engineering, the formation of galvanic couples in the field could be prevented. These methods could include wrapping of pipe laterals that traverse trenches that are to be filled with CLSM, wrapping the repaired pipe in polyethylene or another protective material, using dielectric pipe fittings or couplers to prevent the formation of a galvanic cell, ensuring that pipes are not placed directly on native soils, and other standard methods. Good engineering practice, as has been practiced with conventional soil bedding and backfill materials, can lead to increased use of CLSM such that owners and contractors can achieve faster construction, minimal trench settlement, and reduced corrosion activity of pipelines embedded in CLSM.

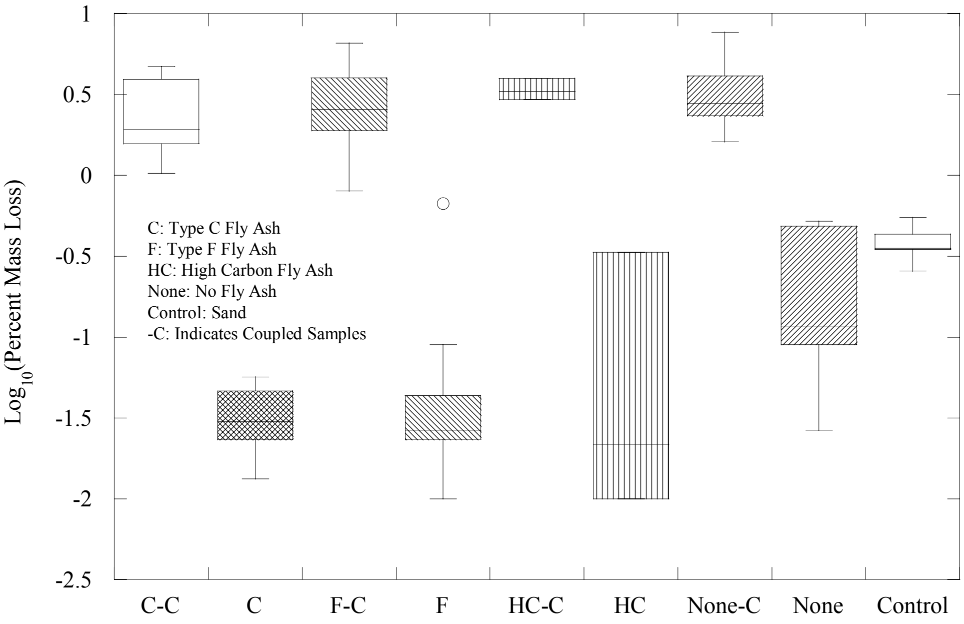

Figure 15 Uncoupled versus coupled log mass loss versus CLSM mixtures containing fly ashes.

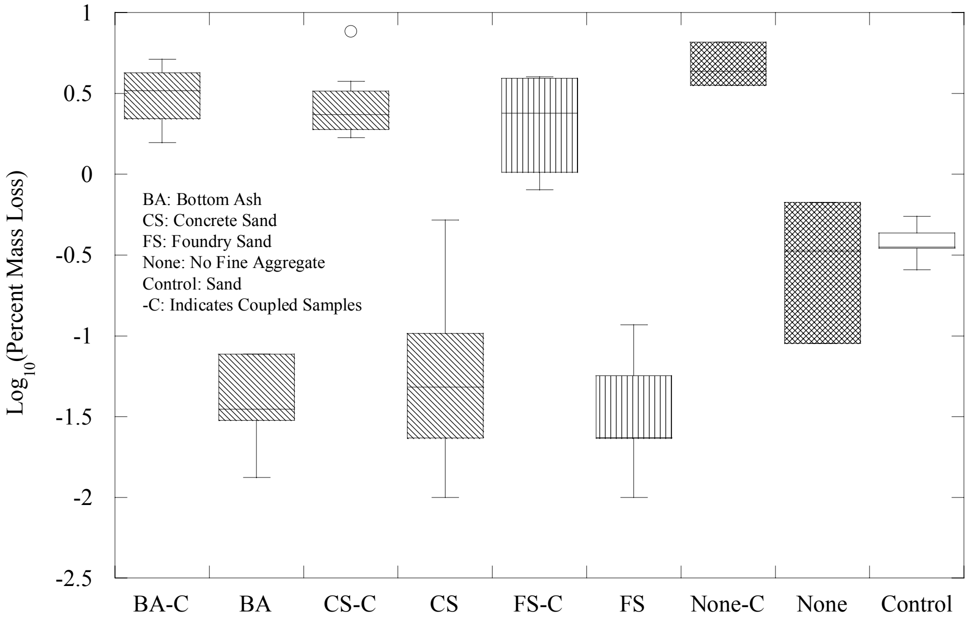

Figure 16 Uncoupled versus coupled log mass loss versus CLSM mixtures containing various fine aggregate types.

3. Phase II – Uncoupled Samples

Figure 17 shows the box plot showing the distribution and the median of the percent mass loss data of the galvanized steel and ductile iron metallic coupons exposed to distilled water and chloride solution. Multiple regression and analysis of variance were performed on the data. The mass loss data were used as the response variable and the environment, fine aggregate type, fly ash type, electrical resistivity, pH, metal type, water cementitious materials ratio, and cement content were used as the explanatory variables.

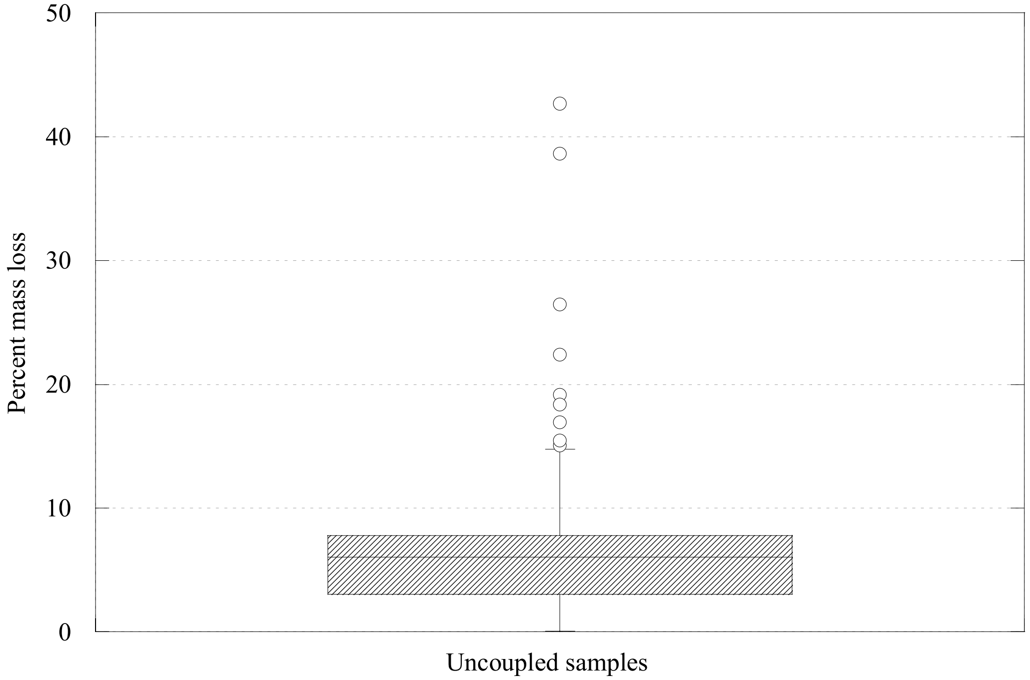

Figure 17 Percent mass loss distribution of metallic coupons

Evaluation of different possible models for coefficient of multiple determination (R^2), the C_p statistic, and the error sum of squares indicated that the best model had a square root of the percent mass loss values as the response variable. This model is shown below:

$$\begin{aligned}\sqrt{\%mass\,loss} &= 4.403 + \alpha_{environment} + \beta_{fine\,aggregate} + \gamma_{fly\,ash} + \delta\cdot\log_{10}(\mathrm{Re}sistivity - \Omega cm)\\ &+ \varepsilon\cdot pH + \phi_{metal\,type} + \varphi_{fine\,aggregate*metal\,type} + \eta_{fly\,ash*metal\,type} + \kappa_{\log_{10}(\mathrm{Re}sistivity)*metal\,type}\\ &+ \lambda_{environment*metal\,type} + \mu_{environment*fly\,ash} + \sigma_{environment*fine\,aggregate}\end{aligned} \tag{4}$$

The model includes:

- The main effects of classification variables; environment, fine aggregate type, fly ash type, and metal type (α, β, γ, Φ).
- The main effects of continuous variables; logarithm of electrical resistivity and pH (δ, ε).
- The interaction effects of classification variables with classification variables; fine aggregate type, fly ash type, and environment with metal type. Fine aggregate type and fly ash type with environment (φ, η, λ, μ, σ).
- The interaction effect of a classification variable with a continuous variable; logarithm of electrical resistivity with metal type (κ).

The parameters defined in the model for the main effects of classification variables represent the expected value of the response variable for different levels of the corresponding classification variable, all other factors being the same. The parameters defined in the model for the main effects of continuous variables represent the amount of change in the expected value of the response variable for each unit change of the corresponding continuous variable, all other factors being the same. The interaction parameters in the model define how the response reacts to one variable based on the value or level of another variable.

Table 8 shows the parameters of the model and their standard errors. The parameters for the main effects and interactions that are not shown in the table are zero. The sign of the estimated parameter shows the type of relationship between the effect and the response value. If the parameter is positive, it indicates a direct relationship for the set values of other parameters of the model.

Figure 18 shows the observed percent mass loss values against the predicted values obtained from the model. In total, 8 of 361 data points, which were extreme outliers after the square root transformation of the data, were not included in the analysis. The analysis indicates that the assumption of a regression analysis that the variance of percent mass loss values is not related to the values of the explanatory variables is satisfied. Investigation of data indicates that there were no influential data points influencing the analysis more than the rest of the data points. The linear correlation coefficient (R) of the model is 84%. The R-value is a measure of how much of the variation of the percent mass loss values are explained by the overall model. The analysis of variance indicates that all of the main effects and interactions included in the model were statistically significant, i.e., all of the effects in the model had a significant impact on the value of the response variable; the square root of percent mass loss. The analysis indicates that the probability of getting the observed impact of effects included in this model on the response variable by chance is less than 1% and this probability is less than 3% for the interaction of environment and fine aggregate type.

Research on the corrosion of metals in concrete has established that high alkaline pore water environment (pH between 12 and 13) of concrete leads to the formation of a passive layer on the metal surface protecting the metal from corrosion (Broomfield 1997). Since CLSM is a cementitious material, it also exhibits an environment with higher pH values compared to traditional backfill materials. The mean pH value measured for the CLSM samples was 9.54 with a minimum of 8.42 and a maximum of 11.56. The mass loss data obtained from the study indicated that pH was one of the statistically significant continuous variables and that the expected square root of percent mass loss decreased with the increasing pH values. These findings are contrary to the point system established by AWWA where points were assigned for high pH values. Figure 19 shows the box plots of square root of percent mass loss values for different pH ranges observed in this study. The pH ranges are built using the 0, 25, 50, and 100 percent quartiles of the data.

Table 8 Parameters and their standard errors of the model

Main effect		**Parameter**	**Standard Error**
Intercept		4.4030	0.6610
Environment (α)			
	Chloride	0.7270	0.2780
Fine Aggregate type (β)			
	Bottom Ash	0.5080	0.1450
	Foundry Sand	0.8300	0.1500
	None	0.3920	0.1910
Fly Ash type (γ)			
	Class C	-0.5030	0.2470
	Class F	0.0776	0.2530
	High-Carbon	0.1250	0.2510
Log$_{10}$(Resistivity) (δ)		-0.0420	0.0858
PH (ε)		-0.2060	0.0422
Metal type (Φ)			
	Ductile iron	-3.3990	0.6300
Interaction effect		**Parameter**	**Standard Error**
Fine Aggregate type & metal type (φ)			
Bottom Ash	Ductile iron	-0.1320	0.1690
Foundry Sand	Ductile iron	1.1960	0.1880
None	Ductile iron	0.2360	0.2330
Fly Ash type & metal type (η)			
Class C	Ductile iron	-0.0130	0.2500
Class F	Ductile iron	0.4380	0.2600
High-Carbon	Ductile iron	0.8800	0.2570
Log$_{10}$(Resistivity) & metal type (κ)			
	Ductile iron	0.5270	0.1170
Environment & metal type (λ)			
Chloride	Ductile iron	0.6030	0.2010
Environment & fly ash type (μ)			
Chloride	Class C	-0.0140	0.2700
Chloride	Class F	-0.5130	0.2760
Chloride	High-carbon	-0.6800	0.2730
Environment & fine aggregate type (σ)			
Chloride	Bottom Ash	-0.3380	0.1640
Chloride	Foundry Sand	-0.4540	0.1690
Chloride	None	-0.2160	0.2330

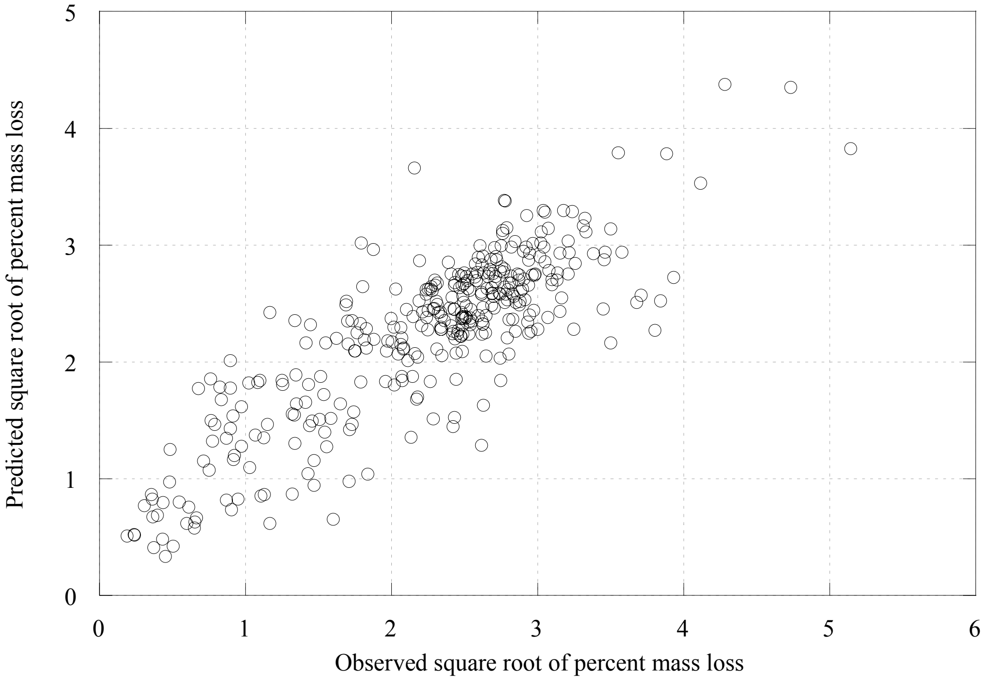

Figure 18 Observed percent mass loss values vs. the predicted values from the model.

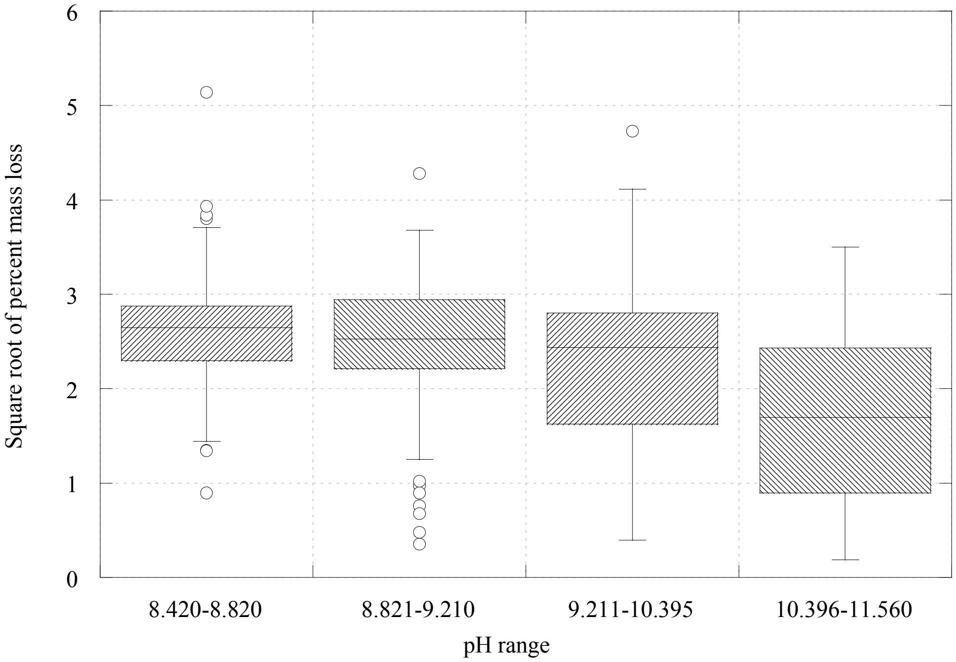

Figure 19 Square root of percent mass loss box plots for different pH ranges.

Comparison of transformed percent mass loss means for the different levels of classification variables was performed using the Bonferroni comparison of means method. The transformed mean percent mass loss values for the samples exposed to chloride solution and distilled water were 2.765% and 2.291%, respectively. The comparison for the two levels of environment indicates that the means are significantly different and the mean of samples exposed to chloride solution is higher. The lower and upper limits of the 95% confidence interval (95% CI) for the transformed mean of percent mass loss of the samples exposed to chloride solution was 2.57% and 2.96%, i.e., there is 95% probability that the true mean is inside this interval. The 95% CI limits for the transformed mean percent mass loss of the samples exposed to distilled water were 2.10% and 2.48%.

Although previous research has indicated that the alkaline environment would lead to passivation of metals, research has also indicated that the presence of chloride ions above a certain threshold can cause depassivation of the metal leading to corrosion (Tuutti 1982). Figure 20 shows the box plot of transformed percent mass loss values of the samples exposed to chloride solution and to distilled water separated by the metal type. It should be noted that the values shown in Figure 20 are for all the samples with different levels of other significant factors of the model.

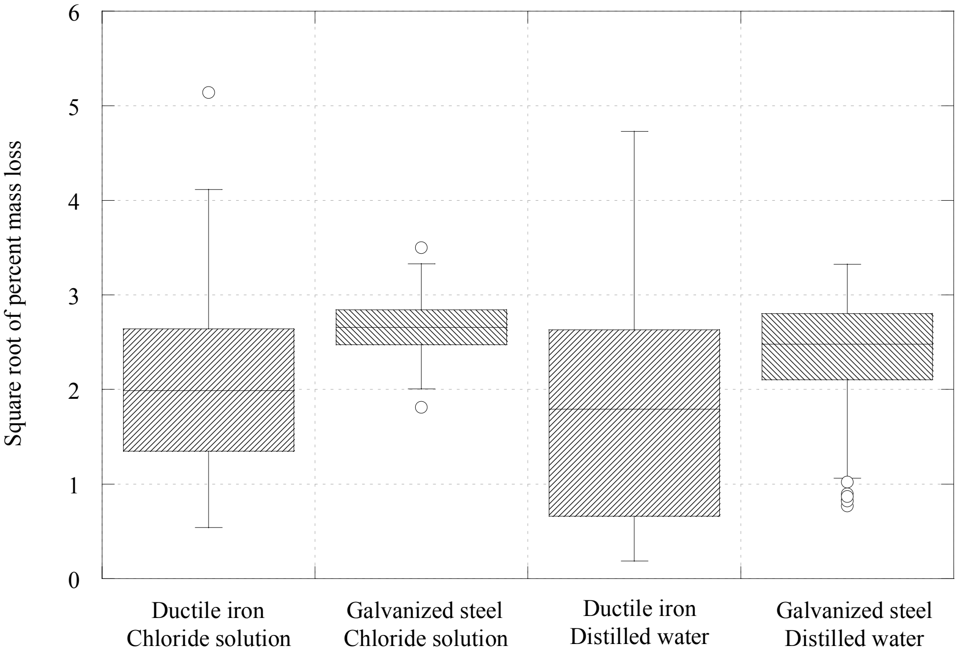

Figure 20 Square root of percent mass loss vs. environment by metal type.

Although there was a significant difference between the mean percent mass loss values of the samples exposed to different environments, analysis indicated a weak correlation between the percent chloride contents and the percent mass loss values among the samples exposed to chloride solution. This could have occurred because the percent chloride contents of these samples were all above the critical chloride threshold value needed to initiate the corrosion, and the actual amount of chloride ions did not have a significant effect.

Resistivity of CLSM samples was a statistically significant continuous variable included in the model. Many researchers investigating the corrosion of metals embedded in soils have noted an inverse relationship between the soil resistivity and corrosion (Peabody 1967, Coburn 1978, Palmer 1990, Chaker 1990, Escalante 1992). Previous research has also indicated that there is a nonlinear relationship between the mass loss of metal coupons embedded in soils and resistivity (Edgar 1989, Palmer 1989). The negative coefficient of logarithm of resistivity in Table 8 indicates an inverse relationship between the resistivity and the percent mass loss values of coupons embedded in CLSM confirming the results of previous research in soils. It should also be noted that the mean resistivity value of CLSM mixtures was significantly affected by the environment.

The transformed mean percent mass loss values for the ductile iron coupons and the galvanized steel coupons were 2.338% and 2.718%, respectively. The comparison of means for the two levels of metal type indicates that the means are significantly different and the galvanized steel coupons exhibited a higher mean square root of percent mass loss. The 95% CI limits for the transformed mean percent mass loss of the ductile iron coupons and the galvanized steel coupons are 2.17% to 2.51% and 2.58% to 2.86%, respectively. Previous research on corrosion of metals in concrete indicates that if the pH value of pore water solution is between 12.2 and 13.3, zinc is covered with a protective film of calcium hydroxyzincate, which protects the underlying steel against corrosion. If the pH value is over 13.2, zinc is in an active state and corrodes. If the pH of the surrounding solution is between 11 and 12, zinc is covered with a porous zinc oxide layer that offers no protection against corrosion (Macias and Andrade 1987). The majority of samples had pH values less than 11 as shown in Figure 21.

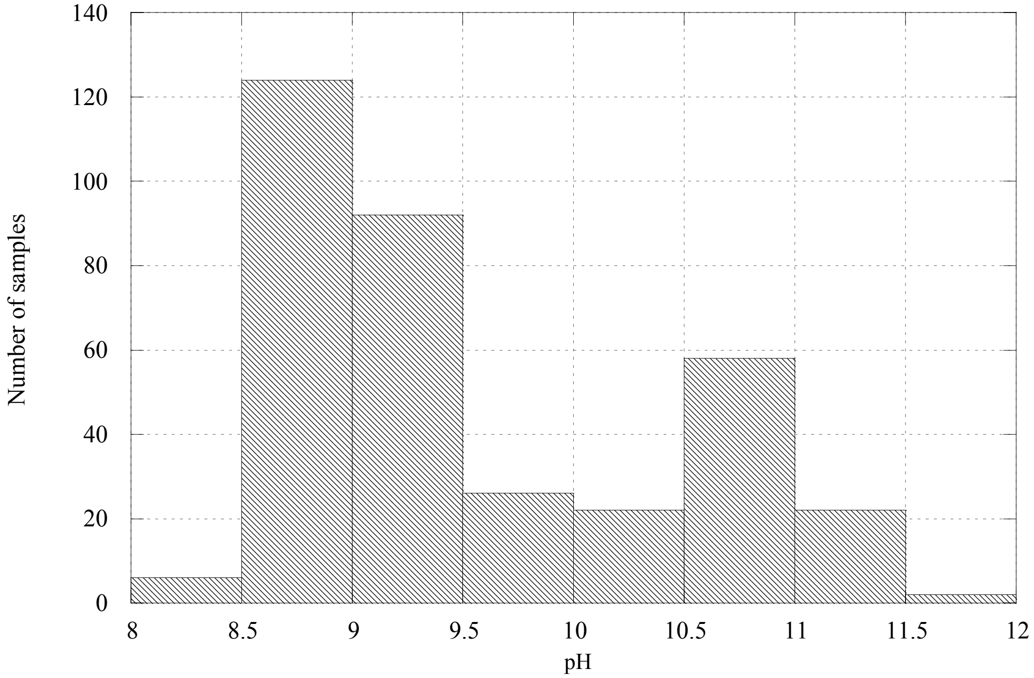

Figure 21 Histogram of pH values of the CLSM mixtures.

Comparison of the transformed mean percent mass loss for the four different fly ash types indicated that only the mean of the samples containing Class C fly ash were significantly different (in this case lower) from the other fly ashes. There was not sufficient evidence to show that the transformed mean percent mass loss values for the other three fly ash types were different. The mean percent mass loss values for Class C, Class F, high carbon, and no fly ash containing samples are 2.074%, 2.631%, 2.816%, and 2.591% respectively. The 95% CI limits for the transformed percent mass loss value of the samples containing Class C fly ash were 1.92% to 2.23%.

Previous studies have reported that some siliceous byproducts with pozzolanic properties may potentially decrease the alkalinity of pore solution in concrete. Parameters such as the alkali content of cement and byproduct and the absorption capacity of calcium silicate hydrate (CSH) like gels for alkalis are believed to be important in determining the effect of byproducts on the alkalinity of pore solution (Lorenzo et al. 1996). Figure 22 shows the box plots for the pH values of samples containing sand as the fine aggregate, separated by fly ash type and cement content.

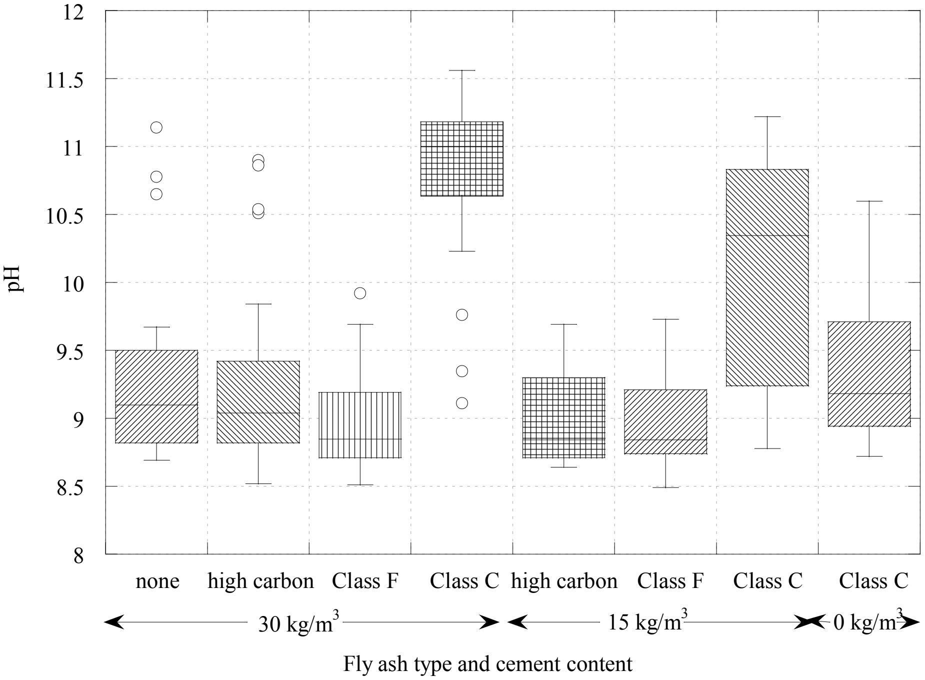

Figure 22 Box plots of pH for sample containing sand as fine aggregate.

Figure 23 shows the box plots for the square root of the percent mass loss values of samples containing sand as fine aggregate, separated by fly ash type and cement content.

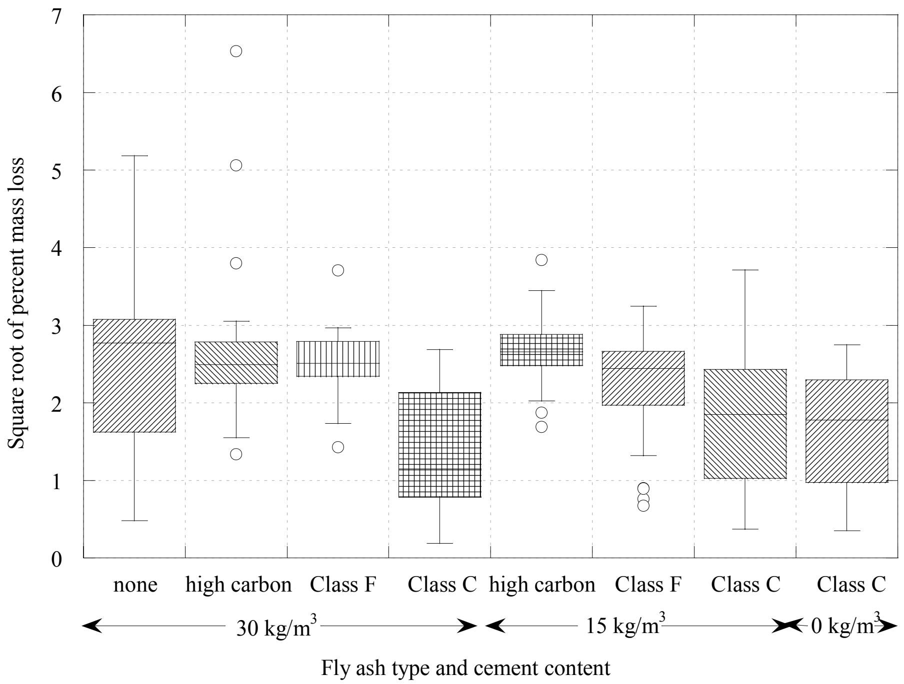

Figure 23 Square root of percent mass loss box plot for samples containing sand as fine aggregate.

The figures show that among the samples with the same amount of cement content, samples with Class F and high-carbon fly ashes have lower pH values compared to the samples with Class C fly ash and samples without fly ash. The figures also show that among the samples with the same cement content, samples with Class F and high-carbon fly ashes have higher percent mass loss values compared to the samples with Class C fly ash. The difference between the percent mass loss values of samples containing Class C and the rest of fly ash types matches the pH difference of the samples. This may indicate that the difference in percent mass loss values is mainly due to the pH difference of the pore solutions of samples containing different types of fly ashes.

Comparison of the transformed mean percent mass loss for the four different fine aggregate types using the same comparison method discussed earlier indicates that there are three distinct groups. Sand and foundry sand are the first two groups and the third group includes bottom ash and samples without fine aggregates. The difference between the mean percent mass loss of samples containing bottom ash and samples without fine aggregates is statistically not significant. The mean percent mass loss values for the sand and foundry sand containing samples are 2.059% and 3.259%, respectively. The mean percent mass loss for the third group is 2.332% and 2.461%, but their difference is statistically not significant. The upper and lower limits for the 95% CI for the transformed mean percent mass loss of sand, foundry sand, bottom ash containing samples and samples without fine aggregates are 1.95% to 2.17%, 3.04% to 3.48%, 2.12% to 2.54%, and 2.17% to 2.76%, respectively.

Figure 24 shows the box plots for the square root of the percent mass loss values separated by the fine aggregate type.

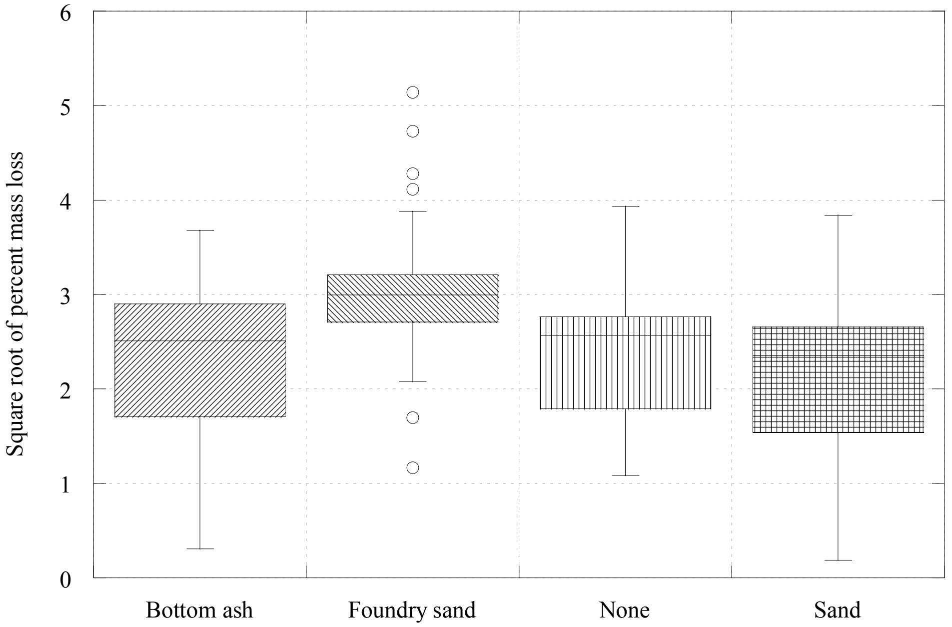

Figure 24 Box plots of transformed percent mass loss separated by fine aggregate type.

Although the samples shown in each box plot have different values of other significant variables determined by the model, the Figure 24 shows that the samples containing foundry sand as the fine aggregate exhibited the highest mean percent mass loss. The pH of spent foundry sand can vary from approximately 4 to 8, depending on the binder and type of metal cast (Johnson 1981) and previous research has reported that some spent foundry sands can be corrosive to metals (John Emery Limited1992).

4. Phase II – Coupled Samples

Figure 25 shows the percent mass loss box plots for the ductile iron and galvanized steel coupons that were embedded in the CLSM and soil sections of coupled samples. Analyses indicate that the percent mass loss values of metallic coupons embedded in CLSM and soil were significantly correlated and the mass loss values of coupons embedded in the soil section of samples were higher compared to the mass loss values of coupons embedded in the CLSM section of samples. Significant correlation of the mass loss values of metallic coupons embedded in the soil and CLSM sections indicate that the corrosion was mainly taking place due to the galvanic coupling between the identical metallic coupons and that the coupons in the two sections of the coupled samples were not corroding independently. Higher percent mass loss values of coupons embedded in soils indicate that these metallic coupons were behaving as anodes in the corrosion reaction. Since the metallic coupons embedded in the soil sections of coupled samples represent the anode, further statistical analysis will be performed on the percent mass loss data of these coupons.

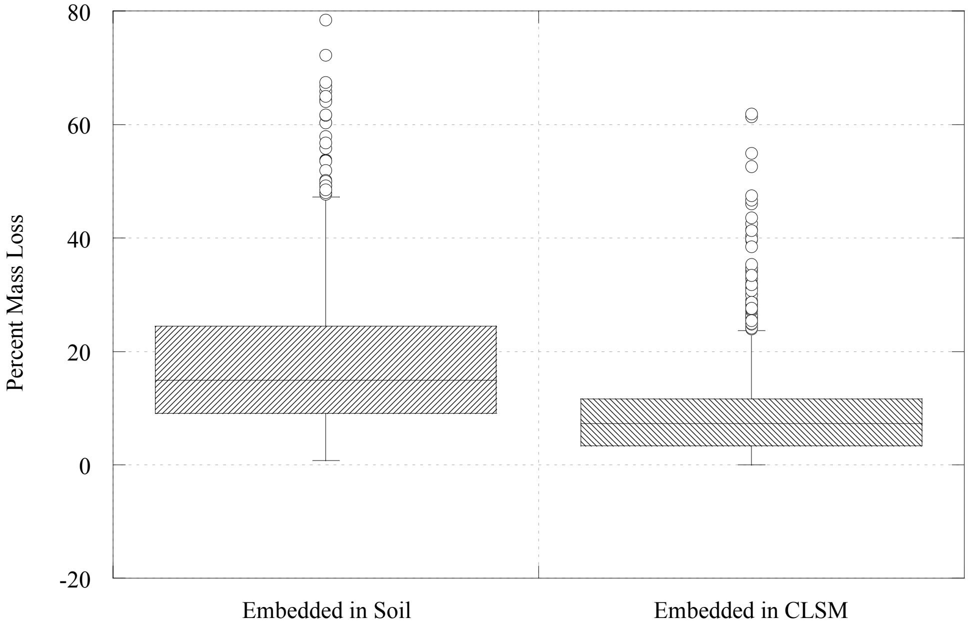

Figure 25 Percent mass loss box plots of coupons embedded in CLSM and soil.

Figure 26 compares the percent mass loss box plots of the phase II uncoupled coupons and the phase II coupled coupons. The figure shows that in the coupled condition the coupons acting as anodes exhibited much higher percent mass loss values compared to the coupons that were tested in the uncoupled condition. The galvanic corrosion of a metal in contact with two different environments is believed to be the main cause of this observed increased corrosion activity (as measured by mass loss).

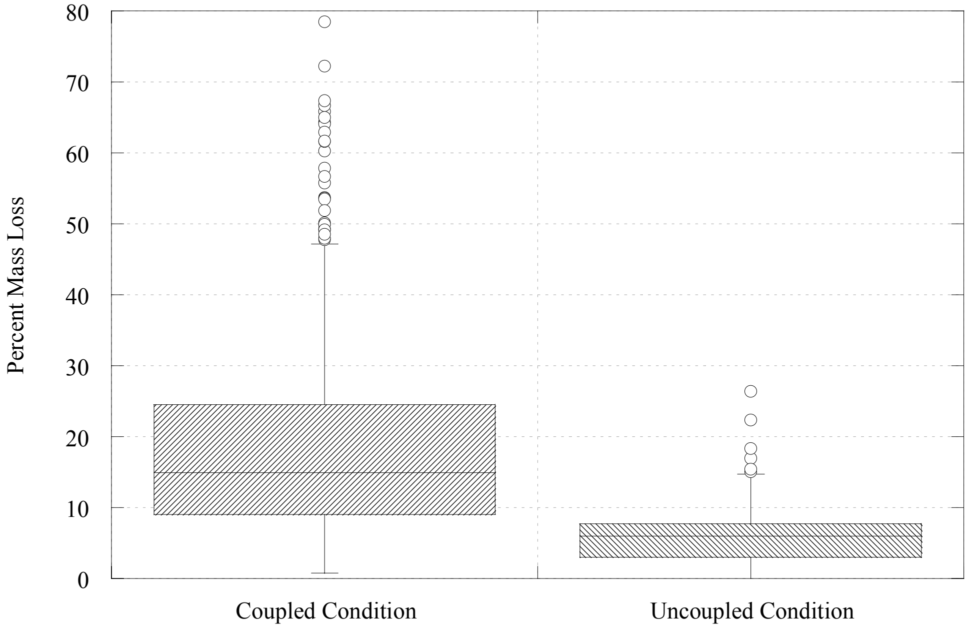

Figure 26 Percent Mass Loss values of coupons embedded in soil section of coupled samples and coupons of uncoupled samples

Multiple regression analysis and analysis of variance were performed on the percent mass loss data of metallic coupons that were embedded in the soil section of the coupled samples. The environment, metal type, soil type, fine aggregate type, fly ash type, resistivity of CLSM, resistivity of soil, pH of CLSM, pH of soil, chloride content of the CLSM, and chloride content of the soil were the regression variables examined. Since in the phase II the pH values of soils were not measured from each sample but a mean value was determined for each soil type using random samples, the soil pH value and the soil type were not independent from each other. To prevent these variables from affecting each other's significance, only the soil type was used in the regression analysis. Analysis using stepwise regression method and evaluation of adjusted multiple determination coefficients (R^2), C_p statistics, and the error sum of squares for different possible models indicated that the best simple model had the logarithm of percent mass loss values (LPML) as the response variable and contained seven terms as shown below:

$$\log_{10}(\%\,Mass\ Loss) = 1.348 + \alpha_{environment} + \beta_{soil\ type} + \delta_{fine\ aggregate} + \varepsilon_{fly\ ash} + \gamma_{metal\ type} + \lambda \cdot pH_{CLSM} + \eta_{environment*soil\ type} \tag{5}$$

The coefficients α, β, δ, ε, and γ are assigned values for the different levels of the classification variables: environment, soil type, fine aggregate type, fly ash type, and metal type, respectively. The coefficient λ is a constant value that is multiplied with the pH value of CLSM. The term η is the interaction term of environment and soil type and η takes different values for different combinations of the levels of these two variables.

Table 9 shows the values of coefficients and their standard errors. The value of the coefficient that is not shown for a level of its variable in the table is zero.

Table 9 Coefficients of variables and their standard errors.

Main effect		Coefficient	Standard Error
Intercept		1.3480	0.1560
Environment			
	Chloride	0.3410	0.0262
Fine Aggregate type			
	Bottom Ash	0.1200	0.0304
	Foundry Sand	0.1350	0.0304
	None	-0.0150	0.0424
Fly Ash type			
	Class C	-0.1670	0.0406
	Class F	-0.2000	0.0406
	High Carbon	-0.1750	0.0399
pH		-0.0270	0.0157
Soil type			
	Clay	0.0202	0.0272
Metal type			
	Ductile iron	-0.0610	0.0187
Interaction effect		**Coefficient**	**Standard Error**
Environment and soil type			
Chloride	Clay	-0.1270	0.0376

Figure 27 shows the observed percent mass loss values against the percent mass loss values obtained from the model. The overall model is statistically significant and the linear correlation coefficient (R) is 57.4%. An R value ranging from about 40% to 60% may be regarded as indicating a moderate degree of correlation (Franzblau 1958). This correlation coefficient is lower compared to the 84% obtained for the model established to estimate the corrosion of phase II uncoupled samples. This indicates that although the investigated CLSM properties and environment factors were good indicators for the amount of corrosion of coupons embedded completely in CLSM, a model built solely from these variables cannot be used to estimate the corrosion of metallic coupons with great accuracy if they are galvanically coupled.

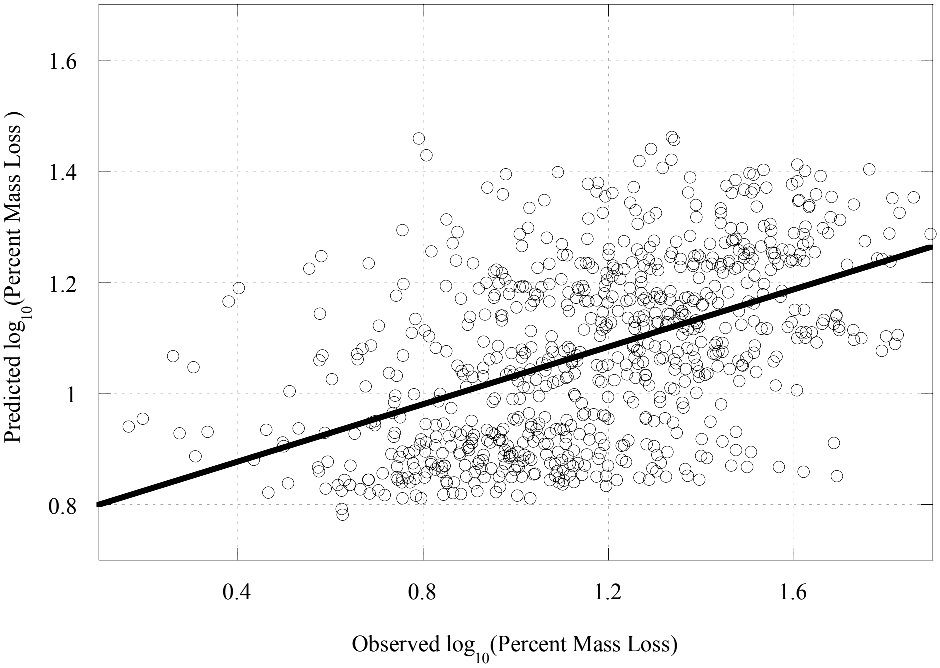

Figure 27 Observed logarithm of percent mass loss vs. the predicted from the model.

It should be noted that all the variables in the model except pH were statistically significant factors at the 99% level, that is, the observed effects of these variables on the expected value of the LPML values were significantly greater than the background level of noise (the probability of the observed effects occurring by chance is less than 1%). The pH of CLSM was significant at the 91% level. All assumptions of regression analysis were checked and satisfied and there were no influential observations and no confounding effects between the variables included in the model. One of the 738 samples was an extreme outlier and was not included in the analysis.

The 95% confidence intervals (95% CI) of pH values obtained from the testing of randomly selected soil samples were 9.33±0.14, 8.08±0.19, 8.17±0.16, and 7.95±0.29 for sand exposed to distilled water, clay exposed to distilled water, sand exposed to chloride solution, and clay exposed to chloride solution, respectively. The pH value of the same sand used in the control samples of the phase I study was measured as 7.46. As noted earlier, pH measurements were performed on soil samples that were actually used for testing in coupled samples and exposed to different environments. The observed higher pH values could be due to the interaction of pore solutions at the CLSM/soil interface of the coupled samples.

The model shows that the type of environment is a statistically significant factor. Tukey's comparison at 95% level of the mean LPML values for samples exposed to different environments indicates that the difference of means is statistically significant. The 95% CI's for the mean LPMLs are 1.36±0.04 and 1.08±0.04 for the chloride solution and distilled water environments, respectively. Figure 28 shows the LPML box plots of the metallic coupons separated by the environment type. There could be two reasons for higher corrosion in the chloride environment. First, previous studies have shown that the existence of chlorides above a threshold level in the vicinity of the steel surface can disturb the passivation of steel surface and increase corrosion (Tuutti 1982). This could be increasing the corrosion on the coupon surface.

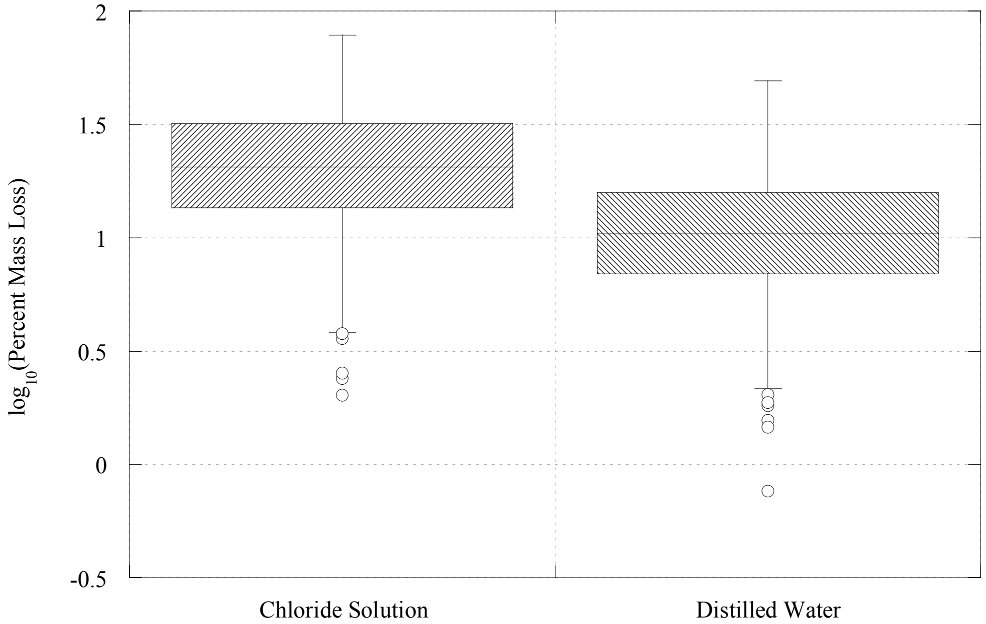

Figure 28 Logarithm of percent mass loss values separated by environment.

Another explanation could be found in the significant correlation between the environment type and the resistivity of CLSM and soil. The CLSM and soil samples exposed to the chloride environment exhibited significantly lower resistivity values that may increase the galvanic corrosion between the embedded coupons of coupled samples by increasing the flow of ions between the coupons. Figure 29 shows the resistivity box plots for soils and CLSM samples exposed to the different environments. The analysis also shows that both the CLSM resistivity and the soil resistivity values were negatively correlated to the LPML values and the correlations were statistically significant.

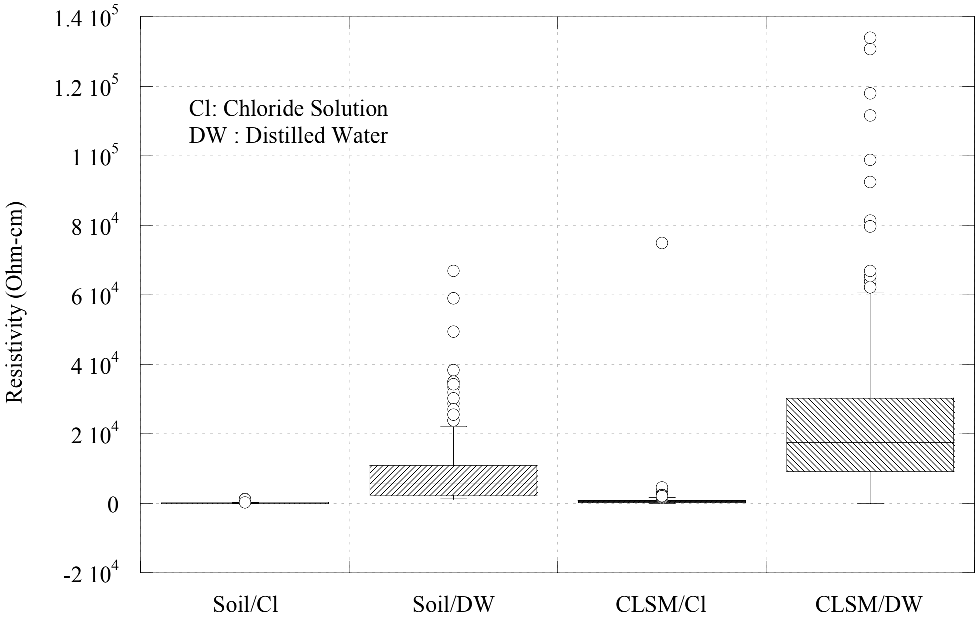

Figure 29 Resistivity box plots of soils and CLSM separated by environment.

The Tukey's comparison at 95% level of mean LPML values of samples embedded in different soil types indicates that the means were significantly different and the mean LPML of coupons embedded in clay was higher. The 95% CI's for the mean LPML values were 1.29±0.04 and 1.15±0.04 for the coupons embedded in clay and sand, respectively. Figure 30 shows the box plots of the LPML values for coupons embedded in clay and sand. Analysis indicates that the resistivity values of clay samples were significantly lower compared to the sand samples exposed to both environments. This could be one of the reasons why the corrosion of coupled coupons embedded in clay were corroding more than the coupled coupons embedded in sand. Figure 31 shows the soil resistivity box plots for coupons separated by soil type and environment. The observed lower mean pH values in clay compared to sand exposed to the same environment could also be another cause for the higher mean LPML values of coupons embedded in clay.

A statistically significant difference in the LPML values was observed between the ductile iron coupons and the galvanized steel coupons. The 95% CI's for the mean LPML values were 1.19±0.04 and 1.25±0.04 for ductile iron coupons and galvanized steel coupons, respectively. Figure 32 shows the LPML box plots of coupons separated by the metal type.

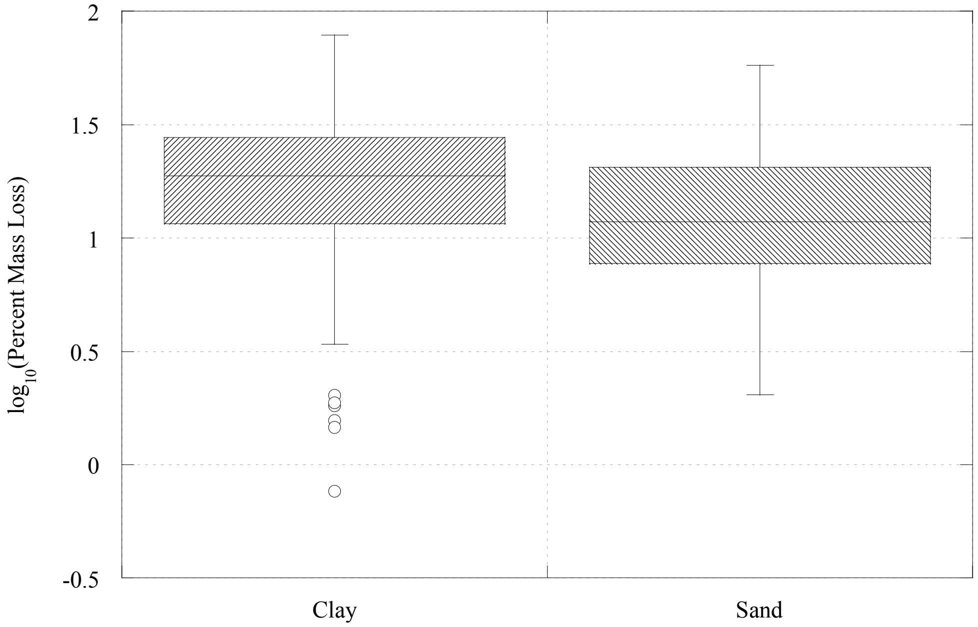

Figure 30 Logarithm of percent mass loss values of coupons embedded in sand and clay.

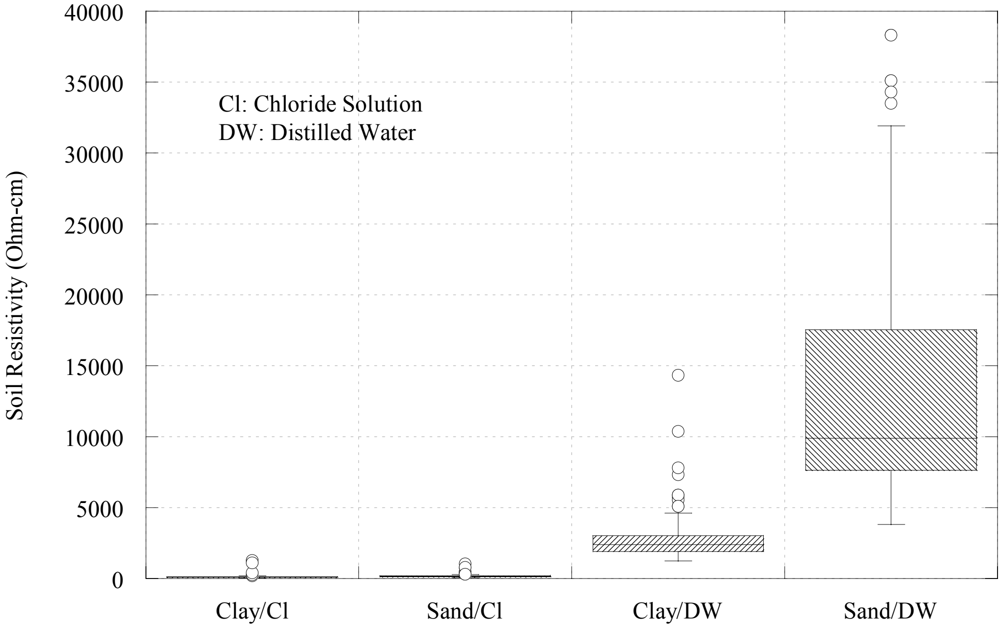

Figure 31 Soil resistivity box plots separated by soil type and environment. (Four extreme outliers of sand in distilled water are not included to show the values using the same scale)

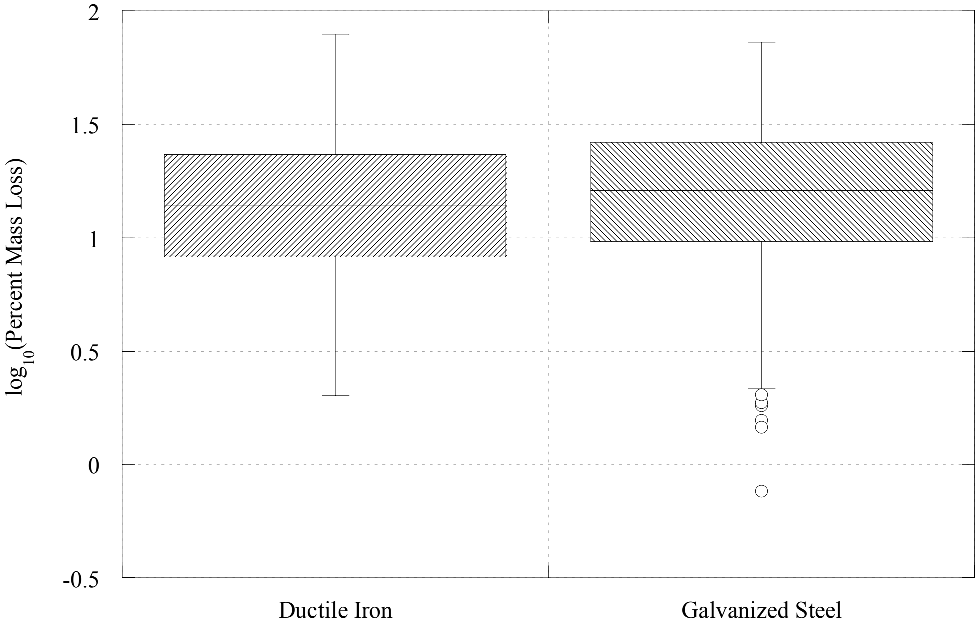

Figure 32 Logarithm of percent mass loss box plots separated by metal type.

These results confirm the results of the uncoupled testing where galvanized steel coupons again exhibited higher percent mass loss values compared to the ductile iron pipe coupons. Galvanized steel has zinc-iron alloy layers on steel with a relatively pure outer layer of zinc. The zinc coating should protect the steel surface from any direct contact with the environment by oxidizing and providing a physical barrier. However, research on galvanized steel cooling towers indicated that the basic zinc carbonate barrier will form on galvanized steel surfaces within eight weeks of operation with water of neutral pH (6.5-8.0). If the galvanized steel is exposed to water with pH greater than 8 for an extended period of time before the zinc carbonate barrier can form, this may lead to the formation of a white, waxy, porous adherent deposit (white rust) which offers no protection (Marley Manual 92-1184A). The Association of Water Technologies (AWT) also stated that during the initial exposure of galvanized steel to water, the pH should be controlled between 6.5 and 8, and chlorides and sulfates should be maintained at levels not corrosive to steel to allow for the formation of a protective oxide layer (AWT 2002). The high alkalinity of CLSM and soil environments (8 or greater) and the observation of white waxy layer during the cleaning of galvanized steel coupons in this study may indicate that the observation of high LPML values of galvanized steel coupons in uncoupled and coupled conditions was due to the disruption of protective oxide layer formation on the galvanized steel surface.

The analysis showed that the fine aggregate type was a statistically significant variable; however, examination of the mean LPML values for different types of fine aggregates showed that no fine aggregate type was significantly different from all of the others. This is contradictory to the results obtained from the phase II uncoupled samples; analysis indicated that metal coupons embedded in CLSM samples containing foundry sand exhibited significantly higher mass loss values compared to the rest of the samples with different fine aggregates or no fine aggregates. The decrease in the significance of the effect of foundry sand is an indicator that in the coupled condition the main driving force of corrosion is the potential difference between the CLSM and soil environments.

The fly ash type was another statistically significant variable in the model. The examination of the LPML values of the metallic coupons in coupled samples with different types of fly ash showed that there were two statistically different sets. The mean LPML value of the coupled samples that contained no fly ash in their CLSM section was statistically significantly higher compared to the rest of the samples (i.e., fly ash reduced the corrosion susceptibility of metallic materials). The 95% CI's for the mean LPML values for samples with Class C, Class F, and high carbon fly ashes were 1.18±0.05, 1.15±0.05, and 1.18±0.05, respectively and the 95% CI for the mean LPML value for samples without fly ash was 1.35±0.09. Results of the phase II uncoupled samples indicated that Class C fly ash increased the alkalinity of the CLSM pore solution and decreased the percent mass loss of metallic coupons. Figure 33 shows the pH values of the coupled samples that had sand as fine aggregates separated by the fly ash type and Figure 34 shows the LPML values for the same groups.

The figures show that Class C fly ash still has the increasing effect on the alkalinity of the CLSM pore solution, however this does not affect the LPML of the coupled coupon embedded in the soil. In this study, the lower LPML values of the samples containing fly ash could be due to the densification of the CLSM structure. The CLSM samples without fly ash could be expected to have a structure with more interconnected pores that can allow the transfer of ions between the coupled coupons more easily. Figure 35 shows the CLSM resistivity box plots of the coupled samples exposed to chloride solution for the same groups shown in Figures 33 and 34 and supports this expectation.

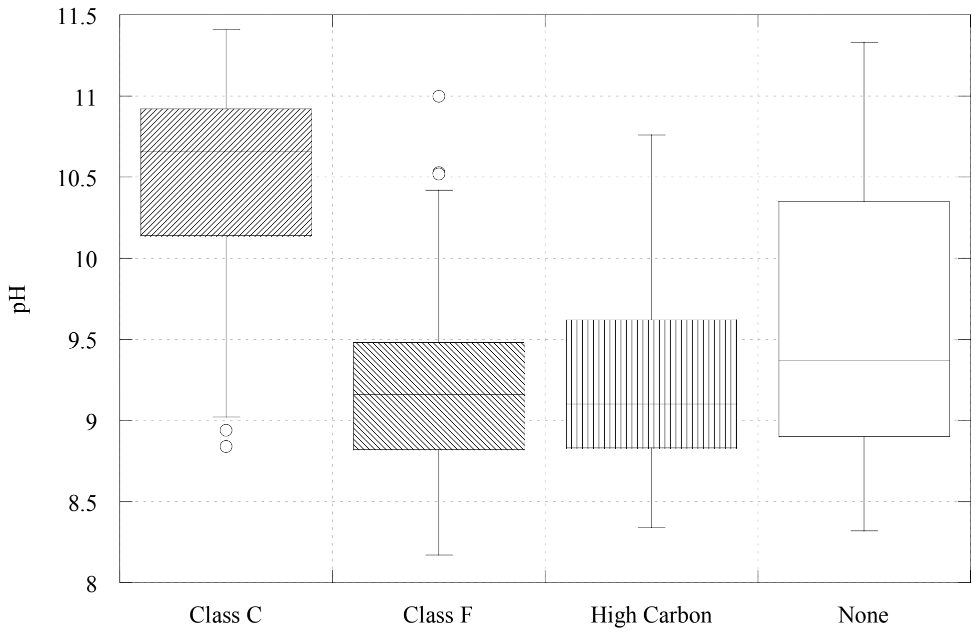

Figure 33 Box plots of pH values for coupled samples with sand as fine aggregate separated by fly ash type.

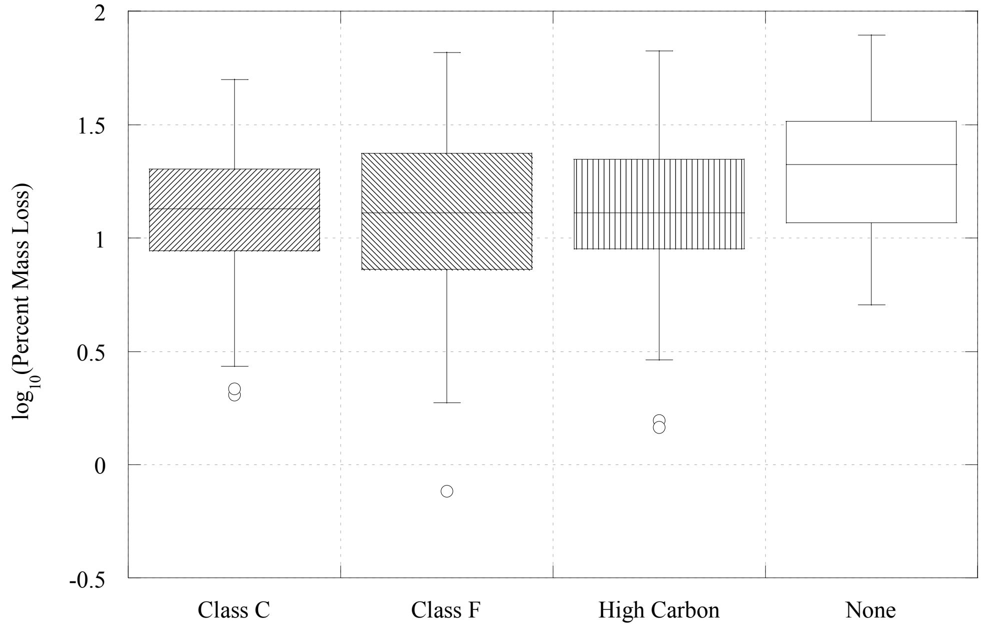

Figure 34 Box plots of LPML values for coupled samples with sand as fine aggregate separated by fly ash type.

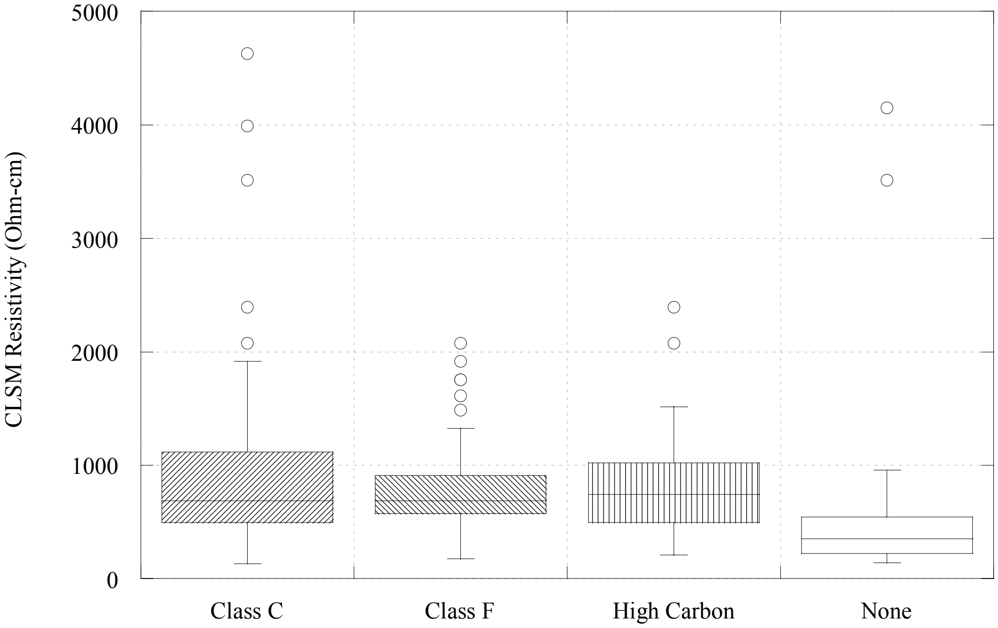

Figure 35 CLSM resistivity values for the coupled samples that have sand as fine aggregate after exposure to chloride solution.

Summary and Conclusions

CLSM has unique characteristics that make it an ideal alternative material for conventional compacted bedding and backfilling materials. Because limited work has been performed on the influence of CLSM on the corrosion of embedded metals, engineers and owners are often reluctant to use CLSM. This research program presented findings on the corrosion of coupled and uncoupled galvanized steel and ductile iron coupons embedded in various CLSM mixtures and exposed to various environments.

Results of the phase I study indicated that the corrosion activity for metallic coupons completely embedded in CLSM was significantly lower than that of ductile iron pipe embedded in sand. CLSM may provide more protection against corrosion initiation and propagation when metallic structures are completely embedded in CLSM compared to compacted sand. Examination of the effects of the constituent materials on corrosion with limited number of samples indicated that there was no significant difference between the fly ash types and the fine aggregate types used in this study. However, the corrosion of metal coupons in uncoupled samples which contained a fine aggregate or a fly ash was lower compared to the coupons in uncoupled samples without a fine aggregate or a fly ash.

Results of the phase II study, where different measurement methods were used for pH and resistivity, indicated that pH and resistivity were significantly correlated factors to the amount of percent mass loss of coupons embedded in CLSM contrary to the findings of the phase I results. The difference in measurement techniques is believed to be the reason for the different results obtained in the two phases. The resistivity and pH measured from separately cast CLSM samples could be better indicator of the inherent properties of the CLSM mixture, however, the values measured directly from the exposed samples in the phase II study exhibited a much better correlation with the measured percent mass loss values. The phase II statistical analysis with higher number of samples detected a difference between the fly ash types and the fine aggregate types used in the study. Metallic coupons embedded in CLSM mixtures with Class C fly ash exhibited lower percent mass loss values compared to CLSM mixtures with other types of fly ashes and without fly ashes. The foundry sand used in this study was found to cause an increased corrosion of metallic coupons compared to the mixtures with other types of fine aggregates. The results of the second phase study also showed that galvanized steel could exhibit a worse corrosion performance compared to ductile iron when exposed to a high moisture and high pH environment like the one examined in this study.

The results of both phases showed that the metallic coupons embedded in the soil section of coupled samples exhibited significantly higher percent mass loss values compared to the coupons embedded in uncoupled samples. Because the main driving force of corrosion was potential difference in the coupled samples, the significance of the factors that affected the corrosion in uncoupled samples was generally lower for coupled samples. Past research has shown that the corrosion activity is increased when metallic materials are placed in soils with significantly different characteristics, and good engineering could prevent this. For instance, various utilities are taking precautions to prevent pipes from traversing dissimilar soils, such as wrapping of pipes or junctions with polyethylene or the use of electrical decouplers. It is logical to conclude that precautions typically taken by engineers to avoid corrosion of metals embedded in dissimilar soils should also mitigate corrosion when CLSM is considered as one of the dissimilar mediums.

References

Association of Water Technologies, "White Rust: An Industry Update and Guide Paper 2002," Retrieved October 13, 2004 from Association of Water Technologies web site: www.awt.org/AWT_WHITE%20RUST%20PAPER_2002.pdf

Abelleira, A., N.S. Berke, and D.G. Pickering, *Corrosion Activity of Steel in Cementitious Controlled Low-Strength Materials vs. That in Soil*. The design and application of controlled low-strength materials (flowable fill). A.K. Howard and J.L. Hitch, Eds. 1998, American society for testing and materials (ASTM): West Conshohocken, PA. 339.

Bhat, S.T. and C.W. Lovell, *Flowable Fill Using Waste Sand: a Substitute for Compacted or Stabilized Soil*. Testing Soil Mixed with Waste or Recycled Materials, ASTM STP 1275. 1997, West Conshohocken, PA.

Bonds, R.W., *Agglite Fly Ash Flowable Backfill*, B. Chin, Editor. 1992, Ductile Iron Pipe Research Association: Birmingham, Alabama. p. letter.

Broomfield, J.P., *Corrosion of steel in concrete*. 1997, London and New York: E & FN Spon. 5-6.

Byfors, K., *Influence of Silica Fume and Fly Ash on Chloride Diffusion and pH Values in Cement Paste.* Cement and concrete research, 1987. **17**: p. 115-130.

CC Technologies Laboratories, Inc., "Corrosion costs and preventive strategies in the United States", report to Federal Highway Administration (FHWA), Office of Infrastructure Research and Development, Report FHWA-RD-01-156, September 2001.

Cady, P. and E. Gannon, *Condition Evaluation of Concrete Bridges Relative to Reinforcement Corrosion*, in *Report No. SHRP-S/FR-92-110 Vol. 8: Procedure Manual*. 1992.

Cao, L.B., B. Wortley, and V. Sirivivatnanon. *Corrosion Behaviours of Steel Embedded in Fly Ash Blended Cements*. in *Durability of Concrete, Third International Conference*. 1994. Nice, France: ACI.

Chaker, V., "Corrosion Testing in Soils – Past, Present, and Future," Corrosion Testing and Evaluation; Silver Anniversary Volume ASTM STP 1000, R. Baboian and S. W. Dean, Eds., ASTM, Philadelphia, 1990, 95-111

Coburn, S. K., "Soil Corrosion," Metals Handbook Ninth Addition, Volume 1 Properties and Selection: Irons and Steels, Bruce P. Bardes, Ed., ASM International, Metals Park, OH, 1978, 725-731

Denison, I.A. and M. Romanoff, *Soil Corrosion Studies.* Journal of Research of the National Bureau of Standards; Ferrous Metals and Alloys, 1946. **44**.

Diamond, S., *Effects of two Danish Fly-ashes on Alkali Contents of Pore Solutions of Cement Fly-ash Pastes.* Cement and concrete research, 1981. **2**: p. 383-394.

Ductile Iron Pipe Research Association, "Ductile Iron Solutions," in *Ductile Iron Pipe News*, Fall/Winter 1994.

Edgar, T.V., *In-Service Corrosion of Galvanized Culvert Pipe*. Effects of soil characteristics on corrosion, V. Chaker and J.D. Palmer, Eds. 1989, American Society for testing and materials: Philadelphia. 133-143.

(EPA), E.P.A., *Back Document for Proposed CPG III and Draft RMAN III*, in *EPA Report EPA530-R-98-003*. 1998, Environmental Protection Agency: Washington, D.C.

Escalante, E., “Measuring the Corrosion of Steel Piling at Turcott Yard, Montreal, Canada- A 14 Year Study,” Corrosion Forms and Control for Infrastructure, ASTM STP 1137, Victor Chaker, Ed., ASTM, Philadelphia, 1992, 339-355

Folliard, K.J., et al., *Controlled Low-Strength Material for Backfill, Utility Bedding, Void Fill, and Bridge Approaches*, in *NCHRP 24-12 Interim Report*. 1999.

Franzblau, A., *A Primer of Statistics for Non-Statisticians*. 1958: Harcourt, Brace & World.

Hoar, T.P. and T.W. Farrer, *The Anodic Characteristics Of Mild Steel In Dilute Aqueous Soil Electrolytes.* Corrosion Science, 1961. **1**: p. 49-61.

Holden, W.R., C.L. Page, and N.R. Short, *The Influence of Chlorides and Sulphates on Durability of Reinforcement in Concrete*. Corrosion of Reinforcement in Concrete Construction, ed. A.P. Crane. 1983, Ellis, Horwood, Chichester. 143-150.

John Elmer Geotechnical Engineering Limited, *Mineral Aggregate Conservation - Reuse and Recycling*. 1992, Aggregate and Petroleum Resources Section, Ontario Ministry of Natural Resources: Ontario, Canada.

Johnson, C.K., *Phenols in Foundry Waste Sand.* Modern Casting, American Foundrymen's Society, 1981(January).

Kozhushner, G., R. Brander, and B. Ng. *Use of Pipe Recovery Data and the Hydroscope "NDT" Inspection Tool For Condition Assessment of Buried Water Mains*. in *AWWA Infrastructure Conference*. 2001: American Water Works Association.

Levlin, E., *Aeration Cell Corrosion of Carbon Steel in Soil: In Situ Monitoring Cell Current and Potential.* Corrosion Science, 1996. **38**(12): p. 2083-2090.

Lorenzo, P., S. Goni, and S. Hernandez, *Effect of fly ashes with high total alkali content on the alkalinity of the pore solution of hydrated portland cement paste.* Journal of the American Ceramic Society, 1996. **79**(February 1996): p. 470-4.

Macias, A. and C. Andrade, *Galvanized steel behaviour in Ca(OH)2 saturated solutions containing SO4= ions.* Cement and Concrete Research, 1987. **17**(2): p. 307-316.

Marley, *White Rust and Water Treatment Manual 92-1184A*. 1992, Marley Cooling Tower Company.

Mozer, J.D., Bianchini, A. C., Kessler, C. E., *Corrosion of Reinforcing Bars in Concrete.* Journal of the American Concrete Institute, 1965. **62**(9): p. 909-930.

Naik, T.R., et al., *Design and Testing Controlled Low Strength Materials (CLSM) Using Coal Ash*. Testing Soil Mixed with Waste or Recycled Materials, ASTM STP 1275. 1998, West Conshohocken, PA.

Okpala, D.C., *Pore Structure of Hardened Cement Paste and Mortar.* International Journal of cement composites and lightweight concrete, 1989. **11**(4): p. 245-254.

Palmer, J.D., *Environmental Characteristics Controlling the Soil Corrosion of Ferrous Piping*. Effects of soil characteristics on corrosion, V. Chaker and J.D. Palmer, Eds. 1989, American Society for testing and materials: Philadelphia. 5-17.

Palmer, J. D., “Field Soil Corrosivity Testing – Engineering Considerations,” Corrosion Testing and Evaluation, Silver Anniversary Volume, ASTM STP 1000, R. Baboian and S. W. Dean, Eds., ASTM, Philadelphia, 1990, 125-138

Peabody, A. W., “Control of Pipeline Corrosion,” National Association of Corrosion Engineers International, Houston, 1967

Romanoff, M., *Underground Corrosion*. 1957, National Bureau of Standards Circular.

Sarhan, H.A., M.W. O'Neill, and P.D. Simon, *Corrosion of Reinforcing Steel in Drilled Shafts with Construction Flaws.* Transportation Research Record, 2002. 1786: p. 96-103.
Spickelmire, B., *Corrosion Considerations for Ductile Iron Pipe.* Journal of Materials engineering and performance, 2002. **11**(July 2002): p. 16-23.
Stern, K., *The Use of Spent Foundry Sand in Flowable Fill in Ohio.* Foundry Management and Technology, 1995. **123**(9).
Tuutti, K., *Corrosion of Steel in Concrete*. 1982, Stockholm, Sweden: Swedish Cement and Concrete Research Institute.

APPENDIX E
IMPLEMENTATION PLAN

This research will be considered successful if the results are used by state DOTs, AASHTO, the US DOT, and others, and if the state of the practice is advanced by the project. During the entire course of the research, the final implementation of the research results was kept in mind. Moreover, as the research developed, refinements to the originally proposed plan were considered. This implementation plan describes several issues and recommended "next steps" that can help to ensure the successful use of the guidance and technology developed under this project.

Products Expected from the Research

The products from this research include the following items:

- A final research report that describes the research, summarizes key data, and provides analyses and conclusions
- Sets of recommended test methods and specifications related to the best use of controlled low-strength material (CLSM)
- A "recommended practice" document that provides general guidance for users on issues to consider in the application of CLSM as backfill, void fill, utility bedding, and bridge approach material

Market for the Research

Several markets for the research exist, including different markets for the different research products. AASHTO, the US DOT, NSF, state and local DOTs, private toll authorities, and utility authorities are probably the largest markets for the results of this research. Any entity that is responsible for "filling in large areas in the ground" has a use for one or all of the products.

The research report and its appendicized study material will also be of interest and use to the research and product-development community, including academics at teaching and research institutions and researchers and engineers at companies that manufacture or promote (e.g., National Ready-Mixed Concrete Association) materials for highway construction. In addition, both DOT staff and private testing firms that are engaged in the quality control or quality assurance of construction materials will find most of the report contents of use.

Potential Impediments to Successful Implementation

The primary impediments to implementation of new or refined construction materials, design guidance, and testing materials are risk, cost, and time. Although the project included significant laboratory and field testing, and despite CLSM having a growing history of successful use, CLSM is a highly variable material whose performance characteristics depend on many, many factors, most of which will vary significantly from project to project. Thus, the use of CLSM introduces additional risk compared to the primary material that it replaces—compacted fill. In addition, CLSM is a designed material that requires complementary laboratory testing and sufficient quality control and quality assurance testing to ensure successful results. These issues have the potential to make CLSM a more costly alternative than compacted fill, especially from a materials-only perspective. However, it should be noted that CLSM may provide time-savings on projects that offset product costs. Finally, the issue of time becomes important, especially in the first several applications of the new guidance and technology, as engineers and construction staff experience a learning curve with the material. Training related to the proper use of the material also consumes time. Finally, there is time required for appropriate sanctioning bodies to review the research results and potentially implement them in AASHTO-, state-, or local-level construction documents.

Leadership in Application of Research Results

Several groups can help to ensure the successful implementation of the research results, including:

- *AASHTO*—As the developer and sanctioning agency for design and construction guidance and documents for state DOT operations, it is important that the appropriate parts of the research results be formally adopted or endorsed through the AASHTO process. As a collective representation of individual state DOTs, AASHTO can also suggest any needed actions (including training) to be developed by FHWA or others. Specifically, the AASHTO Highway Subcommittees on Materials, Construction, and Bridges and Structures have the opportunity to lead the implementation of the refined CLSM technology from this project, both through their promulgating the results (perhaps through informational presentations at their annual meetings) and through formal or informal adoption of the recommended test methods, specifications, and practices in the report.
- *USDOT/FHWA*—FHWA has the ability to assist with implementing new technology in several ways. First, its offices can both assist state DOTs with trial uses of the new/revised procedures outlined in the report and with development of training courses. The National Highway Institute can incorporate information on the new test methods, specifications, and recommended practices into appropriate training courses, if they are needed. The FHWA can also assist with governmental policy or operations changes that may be desirable or necessary to see the successful implementation of the plan. Finally, the FHWA often has programs that can help fund the demonstration of new research, and these are particular useful with respect to assisting with the potential added costs associated with a state DOT's initial foray into the use of CLSM or of the project-developed guidance related to CLSM.
- *International Bridge, Tunnel, and Turnpike Association (IBTTA)*—Toll road authorities are often able to consider accurately the costs and benefits of implementing new technologies that result from research projects. Thus, those

IBTTA members with substantial road or bridge applications for compacted fill may also be excellent testing grounds for the research results.

- *National Science Foundation*—As a major sponsor of research related to the highway infrastructure, NSF may play a significant role in the follow-on science or engineering related to the longer-term improvement of CLSM technology. Additional work on service life prediction, on corrosion-related performance, and on strength and excavatability modeling should be encouraged. In addition, effects of hot weather and large amounts of fly ash on CLSM performance may be better understood with additional research.

Activities Necessary for Implementation

At least the following activities should occur for the research to be implemented:

Technology transfer—the information from this project must get into the hands of the sponsors of transportation research and the highway user and owner communities. This may be best accomplished through the following approaches:

- In late 2006 through mid-2007, consideration should be given to NCHRP, AASHTO, or FHWA support of informational presentations to the AASHTO subcommittees noted above. It will be useful to address all subcommittees, because their roles in projects are notably different. Bridge engineers often specify a technology (such as CLSM) as part of a bridge project or a bridge-approach repair. Geotechnical and materials engineers are probably the most significantly affected, in that they may be the ones provided state-specific specifications and directing or conducting materials tests or project site inspections. Similarly, the construction divisions of DOTs often have significant concerns with how quality control and quality assurance of construction products will be implemented, as well as whether new technologies provide actual improvements to both performance of the constructed facility and the time and cost of construction.
- Promulgation of the results among industry-related groups such as ACI 229, which oversees CLSM and many of the recommended practices and procedures associated therewith.
- Dissemination of the results through technical journal articles that are used by scientists, engineers, and construction contractors. It is worth noting that the project has already provided some information in this way; additional dissemination will help to broadly transfer the knowledge across all aspects of the highway community.

Training—the information in the plan must be presented in a way to ensure correct interpretation and application of the research results, and later, training specifically related to using the tools/methods will be required. FHWA, AASHTO (through NCHRP), or others may consider the development of a brief training program that would highlight the results of the research. Because CLSM is a material already in use, such training should probably strongly indicate which current practices are not necessarily the best and should be changed based on the research findings. The training could be prepared in various formats, either live in-person workshops, videotaped seminars, or even online guidance.

Trial applications—users will have to be convinced to try out the tools/methods. This may require some financial assistance or the allocation of time from their management structure, because the first applications of technology are often more expensive than later ones

"Ownership" of the research results by AASHTO, the US DOT, and state DOTs. This is another reason that informational presentations to AASHTO subcommittees may be important to help ensure that the appropriate groups understand and agree with the importance of the adoption/sanctioning process (and the work related to it) to get the project results formally into AASHTO documents.

Cost information—developing a database of benefits will help the highway community appreciate the usefulness of CLSM. Thought should be given to preparing a standardized cost and time reporting mechanism for states to track their initial experiences with the new CLSM technologies.

Information clearinghouse—an information clearinghouse on experiences with the new CLSM technologies, similar to what was done for metrication in the 1990s or for federally sponsored initiatives, may be helpful. This clearinghouse may become, in effect, a sort of electronic, updated version of the "Special Products Evaluation List" (SPEL) that was popular a decade or more ago.

Judging Progress

A survey of states, perhaps through the AASHTO structure (perhaps a survey of the AASHTO Standing Committee on Highways), regarding their experiences with the research results, should be done at some time after the research results have been "on the street" for sufficient time for multiple projects to have occurred and for the adoption of project recommended guidance by AASHTO. In addition, field test sites mentioned in the research report should be formally followed up on a regular basis to better provide understanding of the issues of corrosion and long-term excavatability.

Applicability of Results to Practice

The deliverables for this project will directly affect operations staff in state DOTs and elsewhere. It will help with providing an alternative material to backfill in a manner that can potentially save significant time. It also serves as a mechanism for using large quantities of materials such as fly ash.